AD-A176 143 SLIDING CONTROL CONCEPT(U) NAVAL SURFACE WEAPONS CENTER 1/1
SILVER SPRING MD R T DRIFTMYER ET AL. 01 OCT 84
NSWC/TR-84-502

UNCLASSIFIED F/G 16/2 NL

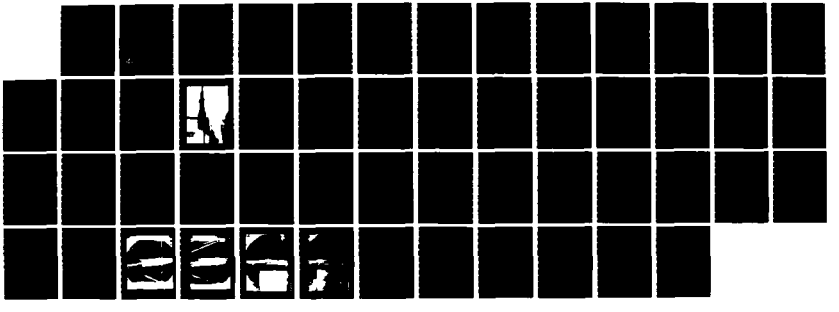

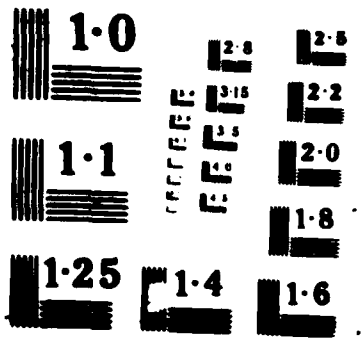
1·0
1·1
1·25
1·4
1·6
1·8
2·0
2·2
2·5
2·8
3·15

NSWC TR 84-502

SLIDING CONTROL CONCEPT

BY R. T. DRIFTMYER L. H. SCHINDEL

STRATEGIC SYSTEMS DEPARTMENT

1 OCTOBER 1984

NAVAL SURFACE WEAPONS CENTER

Dahlgren, Virginia 22448 • Silver Spring, Maryland 20910

UNCLASSIFIED

SECURITY CLASSIFICATION OF THIS P

REPORT DOCUM

AD-A176 143

READ INSTRUCTIONS
FORE COMPLETING FORM

1. REPORT NUMBER
NSWC TR 84-502

ENT'S CATALOG NUMBER

4. TITLE (and Subtitle)
SLIDING CONTROL CONCEPT

5. TYPE OF REPORT & PERIOD COVERED

6. PERFORMING ORG. REPORT NUMBER

7. AUTHOR(s)
R. T. Driftmyer
L. H. Schindel

8. CONTRACT OR GRANT NUMBER(s)

9. PERFORMING ORGANIZATION NAME AND ADDRESS
Naval Surface Weapons Center
10901 New Hampshire Ave
Silver Spring, MD 20903-5000

10. PROGRAM ELEMENT, PROJECT, TASK AREA & WORK UNIT NUMBERS
62766N; ZF66312001; 4K02AD

11. CONTROLLING OFFICE NAME AND ADDRESS

12. REPORT DATE
1 October 1984

13. NUMBER OF PAGES
52

14. MONITORING AGENCY NAME & ADDRESS(if different from Controlling Office)

15. SECURITY CLASS. (of this report)
UNCLASSIFIED

15a. DECLASSIFICATION/DOWNGRADING SCHEDULE

16. DISTRIBUTION STATEMENT (of this Report)
Approved for public release; distribution is unlimited.

17. DISTRIBUTION STATEMENT (of the abstract entered in Block 20, if different from Report)

18. SUPPLEMENTARY NOTES

19. KEY WORDS (Continue on reverse side if necessary and identify by block number)
Control
Missile Control;
Trim,
Stability and Control

20. ABSTRACT (Continue on reverse side if necessary and identify by block number)
A sliding control concept has been investigated as a potential means of trimming a high-performance missile with minimum drag and power penalties. In this concept, control surfaces slide into the exhaust plume of an underexpanded jet and provide stabilizing or control forces by virtue of the flow field encountered in the jet.

Experiments on a convenient sliding control configuration indicate that with jet off the force on the control surface is of a direction and magnitude

DD FORM 1 JAN 73 1473 EDITION OF 1 NOV 65 IS OBSOLETE
S/N 0102-LF-014-6601

UNCLASSIFIED
SECURITY CLASSIFICATION OF THIS PAGE (When Data Entered)

20. (Cont.)

consistent with an elongation of the missile body. The forces imparted by an underexpanded jet acting on the sliding control would depend on the position of the control surface with respect to the jet and on the jet pressure. The ~~jet~~ induced force was not particularly strong for the test configuration, but the scheme could apparently be employed to trim a missile, and, under some circumstances, might provide sufficient force for maneuver.

FOREWORD

The sliding control concept was proposed as a device for maintaining trim of aerodynamically efficient missiles with minimum performance penalty. In this report, experimental data is presented which indicates the potential capability of the concept.

The work was supported by the Naval Surface Weapons Center Independent Exploratory Development Fund.

Approved by:

T. A. CLARE, Head
Strategic Systems Department

CONTENTS

ILLUSTRATIONS

TABLES

CHAPTER 1

INTRODUCTION

A conventional aerodynamic control (Figure 1) for a missile employs a deflected lifting surface, aft of the missile's center of gravity to provide an aerodynamic moment that imparts a rotation to the missile. As a result of this rotation, the missile pitches to an angle of attack.

While this control system is adequate for most purposes, it has drawbacks that can detract from its effectiveness or efficiency. Examples of such deficiencies are:

1. The control force detracts from the missile lift thereby reducing maneuverability and decreasing lift/drag ratio.

2. The control force has a drag component that impairs missile performance.

3. The control force imparts a hinge moment that must be overcome by the control actuators.

4. Aerodynamic controls are ineffective at high altitudes where air density is too low to provide the necessary maneuver forces.

Various devices have been developed to compensate for these shortcomings. For example, the control surface can be moved forward ahead of the missile center of gravity (canard controls). This arrangement is unstable in the sense that the missile will not find a trim position for a given control deflection. Canard controls also induce strong downwash fields on the aft portions of the configuration and may thereby introduce unfavorable nonlinear aerodynamic characteristics. However, since the lift provided by canard controls is in the desired direction, they are sometimes used on highly maneuverable missiles in spite of the aforementioned drawbacks.

Thrust vector controls are employed on some missiles to provide large control moments, even outside of the atmosphere. Of course this type of control is not effective unless the engine is operating. Also, high driving forces and heavy equipment are usually required to push the exhaust nozzles to the desired position. In addition, a loss in performance will be incurred when the thrust vector is not in the flight direction.

Another possible control configuration, also depicted in Figure 1, is a lifting surface arranged to slide into the exhaust of the missile's propulsion

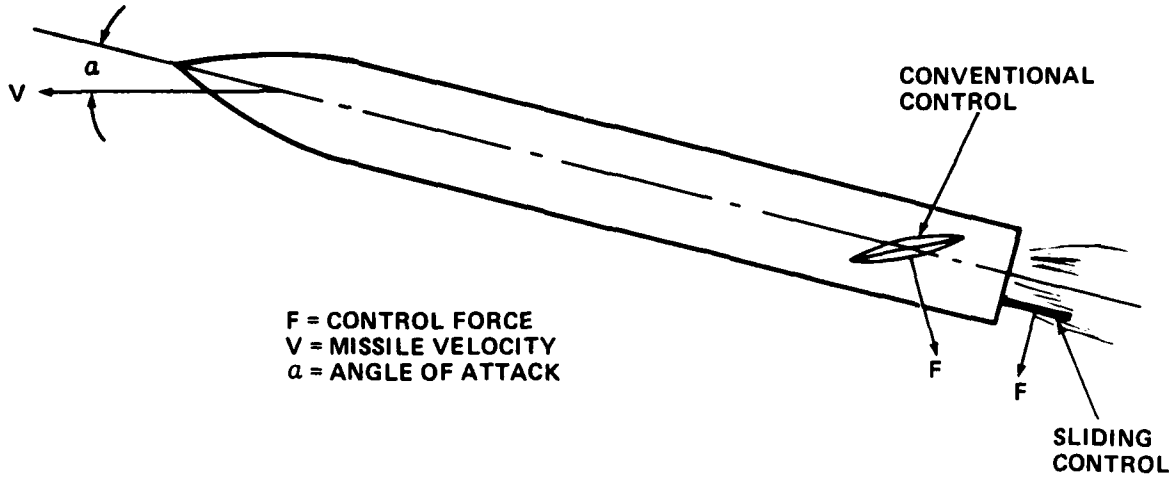

FIGURE 1. CONVENTIONAL MISSILE AERODYNAMIC CONTROL AND CORRESPONDING SLIDING CONTROL

jet. As can be seen in the figure, such an arrangement would have a reduced drag penalty for a given control force.

In this report, an investigation of a sliding control concept will be described. Figure 2 shows a pair of sliding controls mounted on the base of a missile designed for high lift/drag ratio. The control surfaces shown in this figure are located near the exhaust of an underexpanded jet. The controls slide in and out of a slot in the body base to adjust the amount of moment that they provide. They move together to produce a pitching moment and differentially to generate yaw and roll. Other arrangements, such as a square formed by four surfaces, could be employed depending on the desired control forces.

The concept will be described more fully in the next chapter of the report.

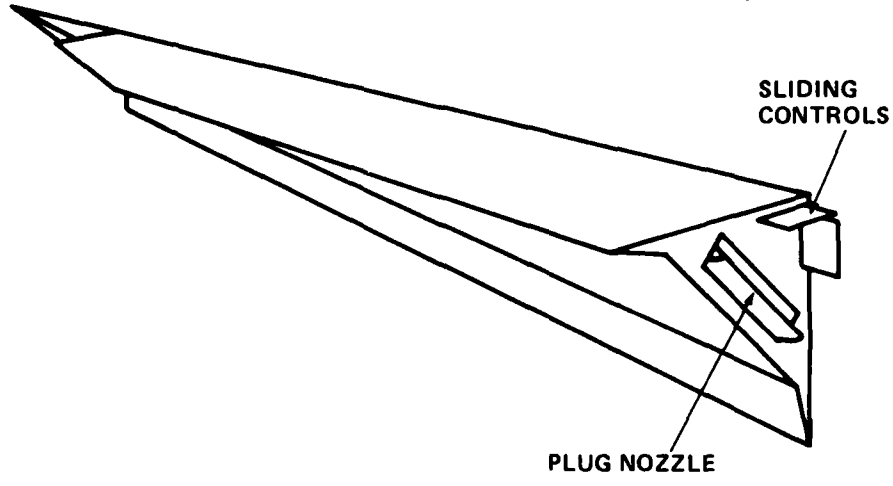

FIGURE 2. SLIDING CONTROL CONCEPT ON HIGH-PERFORMANCE MISSILE

The performance of the concept was examined experimentally in a supersonic wind tunnel test of a convenient configuration. The test conditions are described in Chapter 3, and the results of the test are presented in Chapter 4. In the final chapter, potential applications of the concept are described in light of the test results.

CHAPTER 2

DESCRIPTION OF SLIDING CONTROL CONCEPT

As indicated in Figure 3, the resultant pressure force on a sliding control acts normal to the control surfaces and has no axial force component. Consequently this control system has the potential for providing a given trimming moment with less drag penalty than a conventional control; especially advantageous for vehicles designed for high lift/drag ratio. The sliding control achieves this advantage by its extreme rearward location which means that a small force provides the required control moment, as well as its lack of an axial force component of pressure. The direction of the force depends on the location of the control surfaces with respect to the exhaust jet. If the control is above the exhaust (assuming that the force imparted by the impinging jet exceeds that from the flow on the external surface of the control), then the force will be upward, if below the jet, it will be downward. With the vehicle in its normal trim attitude, the controls would be partially extended. They would slide in or out to increase or decrease the control moment to maintain trim. Whether they can also provide sufficient torque to manuever the missile depends on the required moments and the forces on the control surfaces.

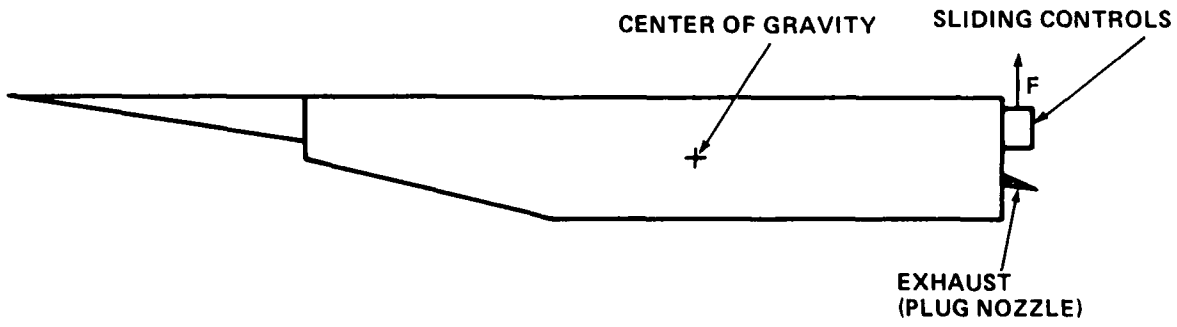

FIGURE 3. GEOMETRICAL ARRANGEMENT OF SLIDING CONTROLS

This control device has the further potential advantage of requiring little actuator force because its motion is opposed only by friction which can be made small by good bearing design.

Like thrust vector controls, the system as visualized here operates only when the jet engine is functioning. However, since it would normally sustain a force even without the jet, it could be designed to operate with no engine thrust.

Wind tunnel measurements were made to determine the magnitude of force which this type of control might be expected to generate. The control force will depend on the geometry of the configuration; hence any measurements are strictly applicable only to the configuration that is tested. Since this investigation addresses no one particular application, the cylindrical control geometry shown in Figure 4 was selected for manufacturing and test convenience. The results are to be interpreted as indicative primarily of the general performance of the concept.

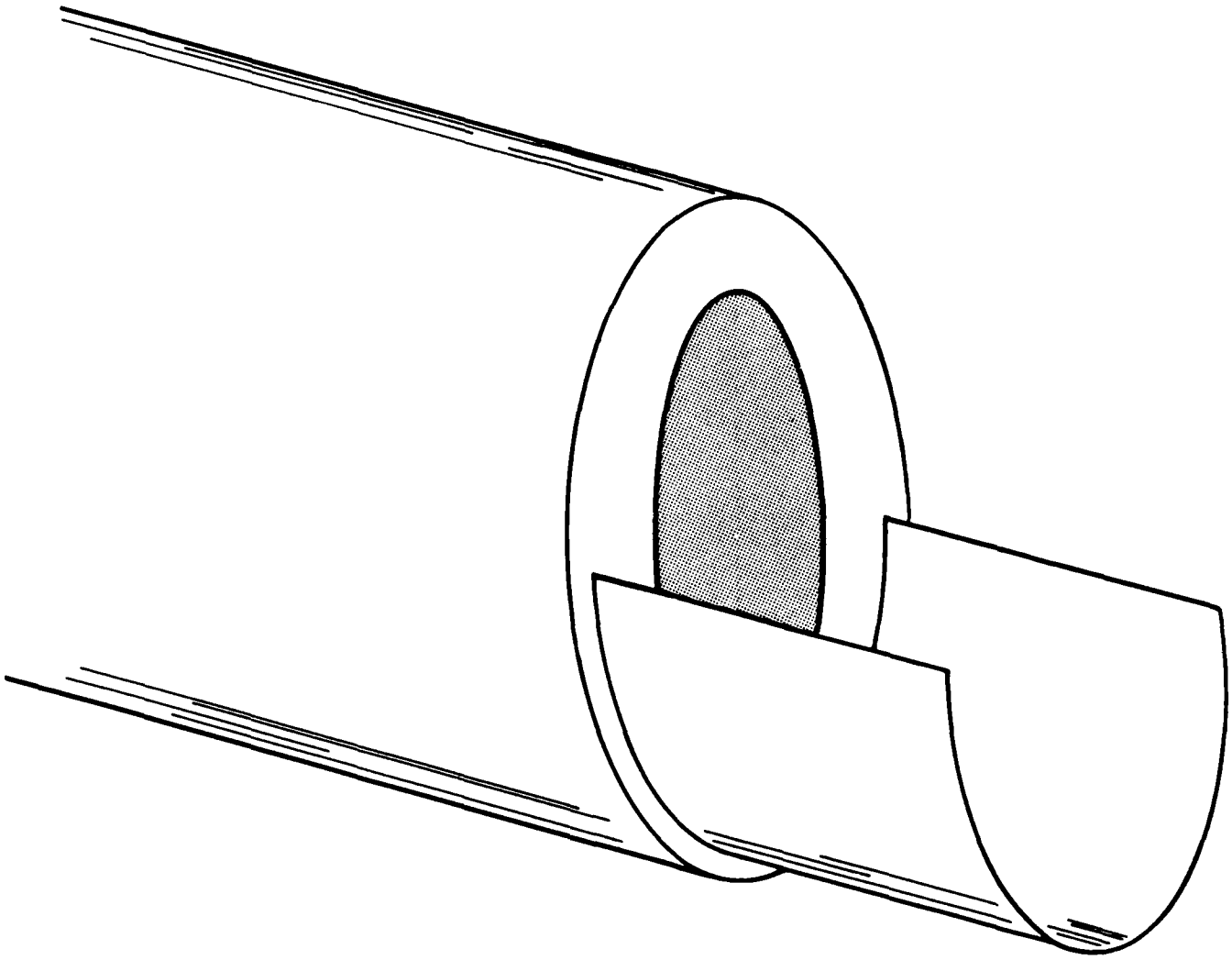

FIGURE 4. CONTROL CONFIGURATION INVESTIGATED

CHAPTER 3

WIND TUNNEL TEST

MODELS

The sliding control geometry consists of a thin half-circular cylinder extending from the base of a circular missile body, as shown in Figure 4. However, the forces on the outside of the control were measured first in a Mach number 2.27 flow, but with no jet. Then, air was supplied to a circular nozzle simulating the exhaust jet impinging on the inner surface of the control with no external flow. Thus, it was assumed that, for the purposes of this experiment, the flows on the interior and exterior surfaces of the control were entirely independent of each other.

On the basis of this assumption, the external control surfaces were modeled as shown in Figure 5. The basic configuration is a blunted cone-cylinder body of length 16.091 in. and diameter 2.75 in. incorporating a 9.065 in. nose. Three semicircular sections could be added simulating control extensions from 0 to 1.5 in.

Forces were measured on the model with 0, 1, 2 and 3 extensions attached. Pressure measurements on interior surfaces of the extensions (as well as on the base of the body) permitted calculation of the magnitude and location of the normal force acting on the external surfaces of the control in its three simulated positions. A photograph of the complete configuration mounted in the wind tunnel is shown in Figure 6.

The model used to determine the forces on the internal surface of the control is depicted in Figure 7. It consists of a cylindrical support housing a conical nozzle. The area ratios are chosen to produce a jet Mach number of 4 at the exit. As in the external surface model, three semicircular extensions can be added to simulate various control positions.

This configuration was mounted in the wind tunnel test section for convenience. The test section was evacuated; then high pressure air was introduced into the nozzle, and pressures on the internal control surfaces were measured as a function of jet pressure ratio.

WIND TUNNEL AND INSTRUMENTATION

All of the force tests were conducted in Supersonic Tunnel No. 2 of the Naval Surface Weapons Center at a free stream Mach number of 2.27. The upstream stagnation pressure was approximately 18 psi except for one run at about 10 psi.

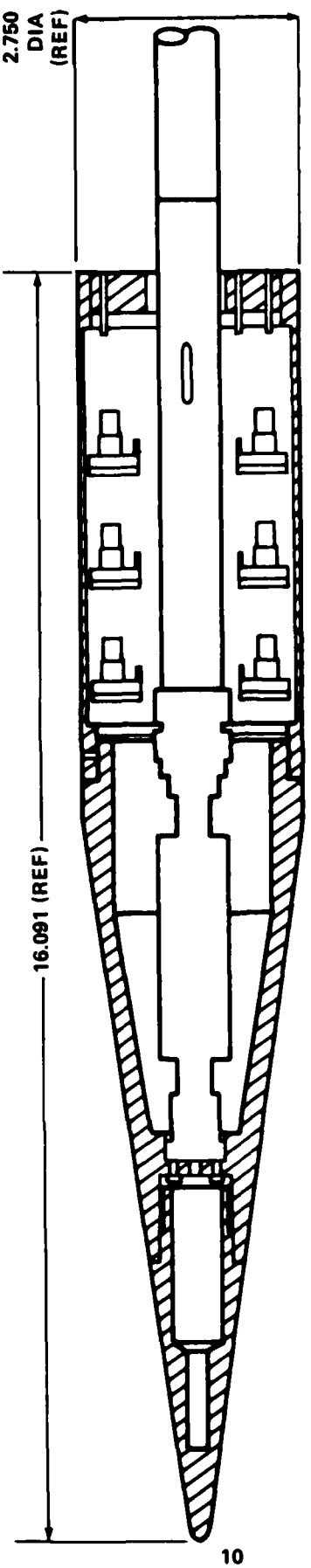

FIGURE 5. MODEL WITH EXTERNAL CONTROL SURFACES

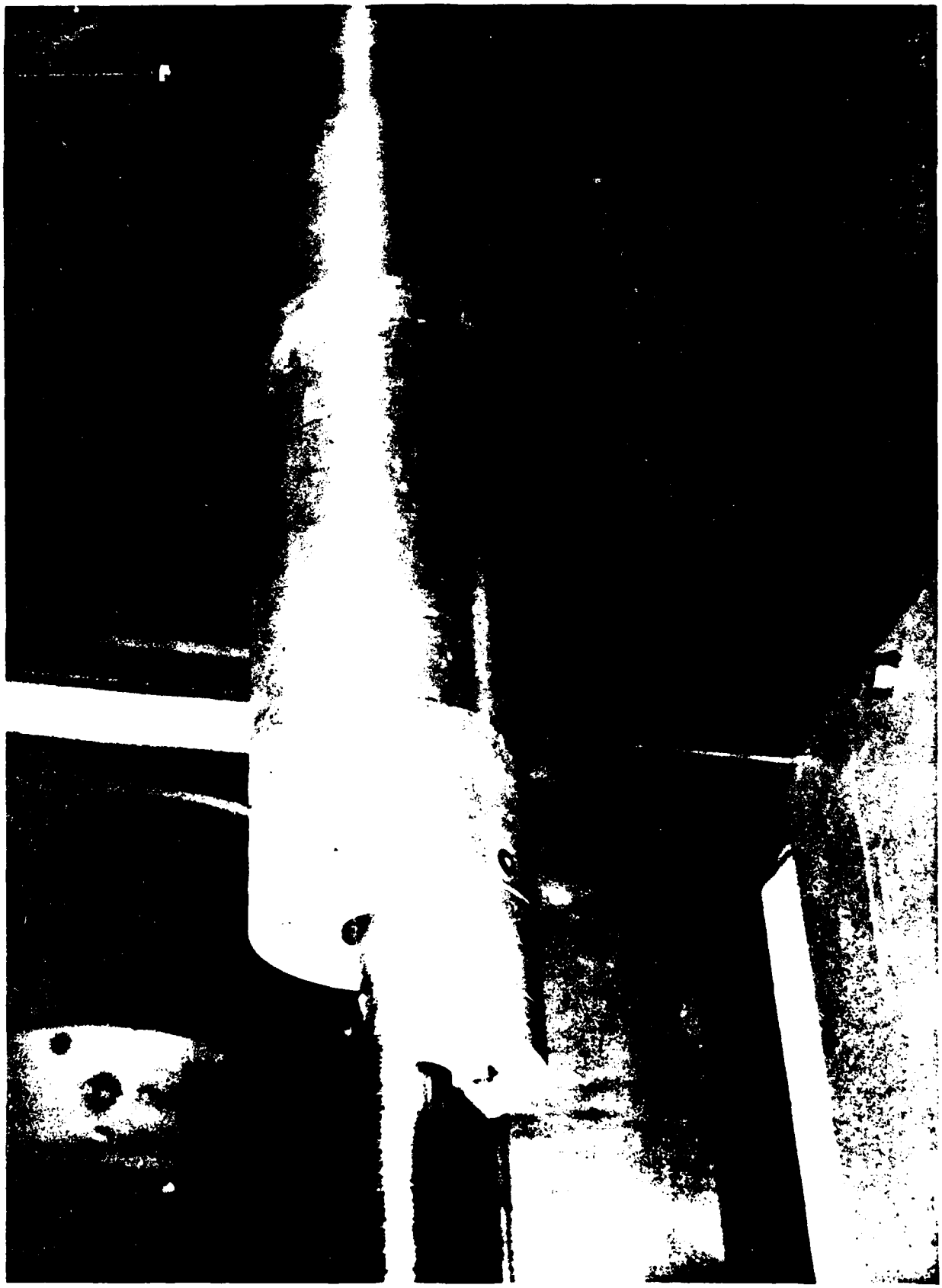

FIGURE 6. FORCE MODEL IN WIND TUNNEL

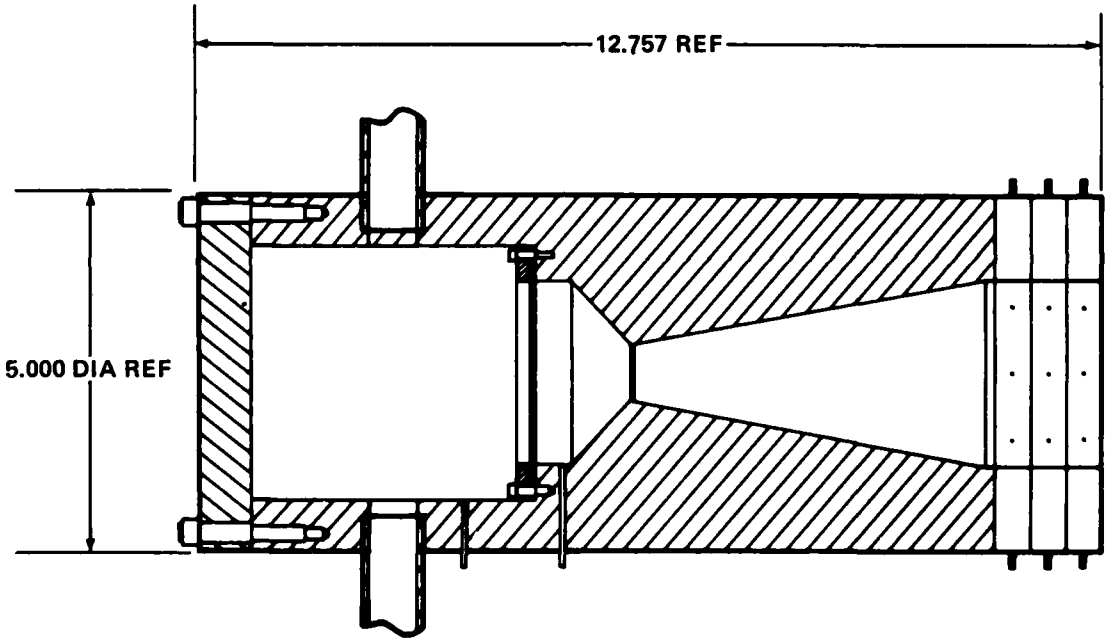

FIGURE 7. CUTAWAY VIEW OF MODEL WITH INTERIOR CONTROL SURFACES

Normal force, axial force and pitching moment were measured by a strain gage balance as the model pitched through angles of attack from about -6° to +6° (corrected for sting deflection). Pressures were measured in the 11 locations shown in Figure 8a using solid state "Microswitch" transducers. Because of faulty connections, the readings from taps 5 and 6 were erroneous and were replaced in the data reduction by the data from symmetrical taps 3 and 8 respectively.

On the jet model, pressures were measured at the locations shown in Figure 8b as well as the ambient pressure in the test chamber and the jet pressure in the model upstream of the nozzle contraction.

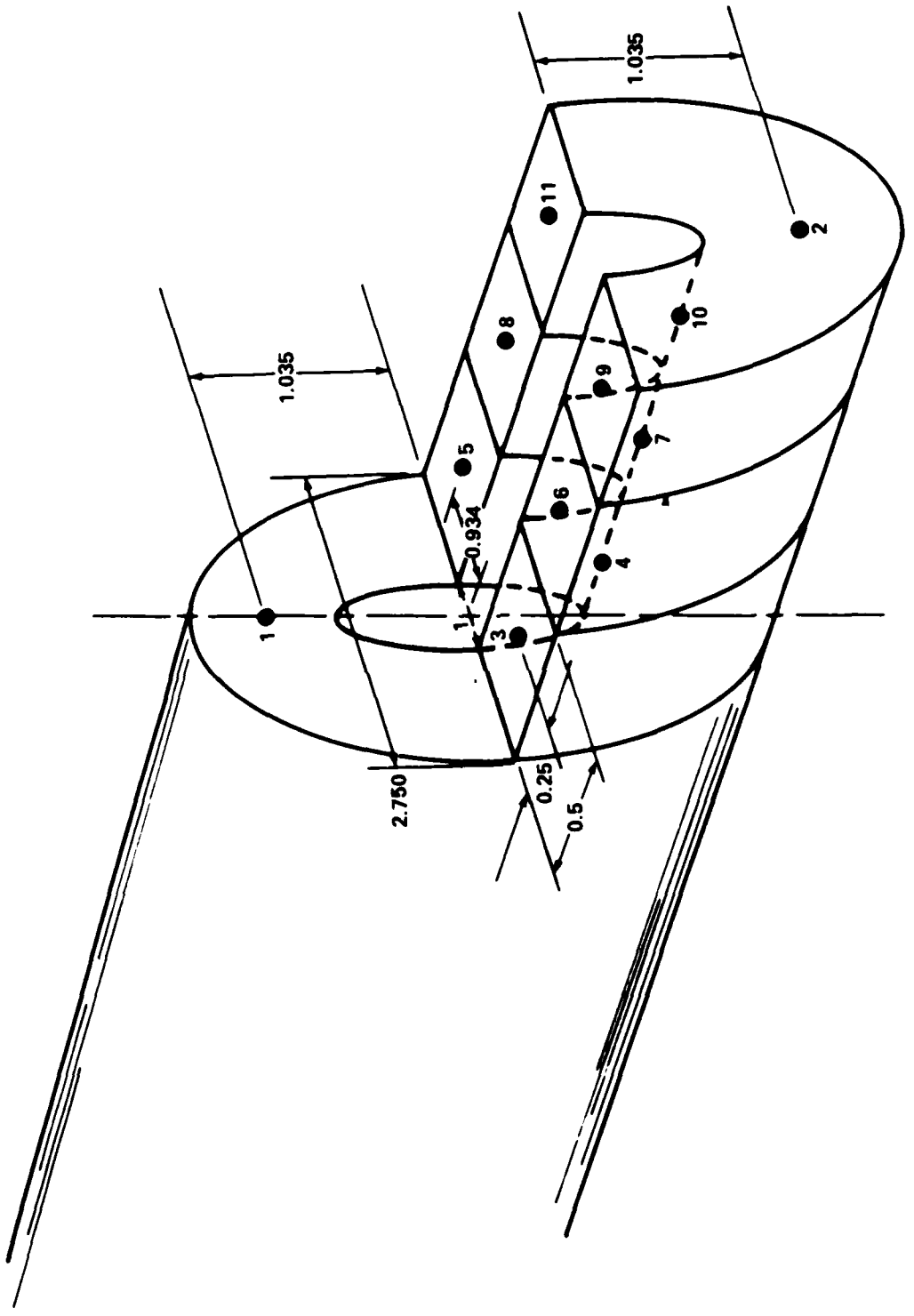

FIGURE 8a. PRESSURE TAP LOCATIONS ON FORCE MODEL

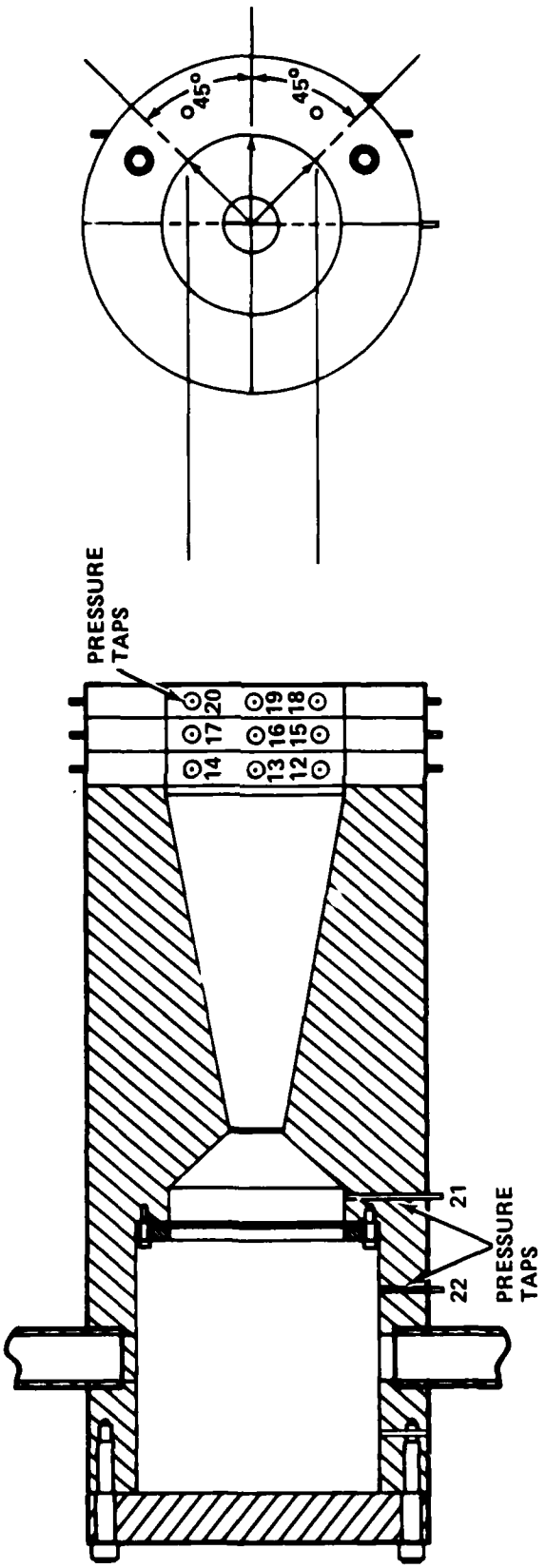

FIGURE 8b. PRESSURE TAP LOCATIONS OF JET MODEL

CHAPTER 4

EXPERIMENTAL RESULTS

RUN SCHEDULES

Two sets of data were acquired. The run schedule for the force tests is shown in Table 1, while the jet test schedule is given in Table 2.

Each force test run consisted of a sweep through angles of attack from -6° to about +6° (or 10°). In each jet test, the pressure in the model chamber was brought up to about 60 psi in five to ten seconds. Meanwhile, the ambient pressure increased as air came into the test chamber faster than it was pumped out. The ambient pressure continued to increase for five to ten seconds more.

TABLE 1. FORCE TESTS (M=2.27)

RUN NO.	CONFIGURATIONS	P_o(PSI)	ANGLE OF ATTACK
0	body alone	9.5	-6° to +10°
1	body alone	18.2	-6° to +6°
2	body +1 control extension	18	-6° to +6°
3	body +2 control extensions	18	-6° to +6°
4	body +3 control extensions	19.7	-6° to +6°

TABLE 2. JET TESTS

RUN NO.	CONFIGURATION	$\frac{P_{JET}}{P_\infty}$
10-16	jet only	5-40
20,21	jet + 1 control extension	5-40
30,31	jet + 2 control extensions	5-40
40-42	jet + 3 control extensions	10-35

DATA REDUCTION

Force Tests

The force measured by the strain gage balance on each configuration is an integration of the pressures over the area of the model plus a friction contribution to the axial force. The pitching moment is an integration of the pressure forces multiplied by their moment arms including contributions from any asymmetrical axial loads. What is desired is the normal force on the external surface of the simulated control and its point of action along the model axis. The control force is obtained by subtracting the body alone normal force from the force on the body plus control extension then deducting the force due to the integrated pressures acting on the inside of the control extension. Expressed in coefficient form, the normal force on the outside of the simulated control is:

$$C_{N_o} = C_{N_T} - C_{N_B} + \frac{1}{A_{REF}} \int C_p dA$$

where C_{N_o} = normal force coefficient on outside of control extension,

C_{N_T} = measured normal force coefficient on body plus control,

C_{N_B} = measured normal force coefficient on body alone.

C_p = pressure coefficient on inside of control extension = $\frac{p}{q_\infty}$

p = measured pressure (absolute)

q_∞ = free stream dynamic pressure

A_{REF} = reference (base) area = 5.9396 in^2

The integration is performed by summing up the products of the measured pressure coefficients multiplied by the area projected on a horizontal plane in body coordinates associated with each pressure tap. The outer pressure taps shown in Figure 8a are assumed to apply to the flat area of the extension Block (.4375 in^2-each) while the center pressure tap applied to the center area (.5 in^2).

The pitching moment provided by the control is found in a similar manner. Moments are measured about the nose of the model.

$$C_{m_o} = C_{m_T} - C_{m_B} - \frac{1}{A_{REF}\ L_{REF}} \left[\int C_p \quad X dA - \int \left(C_{P_b} - C_{P_c} \right) Y dA \right]$$

C_{m_o} = pitching moment coefficient due to force on outside of control extensions

C_{m_T} = measured pitching moment coefficient on body plus control extensions,

C_{m_B} = measured pitching moment coefficient on body alone

X = axial distance from moment center to center of control extension

C_{p_b} = measured base pressure coefficient on exposed body

C_{p_c} = measured base pressure coefficient on control extension

Y = vertical distance in body coordinates to the centroid of the base of the control extension = .640 in

A_b = base area of control extension = 2.5771 in^2

L_{REF} = moment reference length = 16.091 in.

Jet Tests

The pressure force on the internal contour of the control extensions is determined by integration of the measured pressures

$$C_{N_I} = \frac{-1}{A_{REF}} \int C_p dA$$

Here C_{N_I} = normal force coefficient on interior surface of control extension

Cp = pressure coefficient on inside of control extension = $\frac{p}{q_\infty}$

p = measured pressure

p_{JET} = upstream pressure in jet model

p_∞ = ambient pressure in force tests

q_∞ = dynamic pressure associated with corresponding force test.

Similarly, the pitching moment contribution is

$$C_{m_I} = \frac{1}{A_{REF}\, L_{REF}} \int x C_p dA$$

where

x = distance to pressure tap from reference stations (body nose)
L_{REF} = body length 16.091 in.

The integrations indicated by the equations for C_{N_I} and C_{m_I} are performed by adding the products of measured pressure times associated projected area. The projected area over which each pressure is assumed to act is taken as 1/3 the inside diameter of the control extension (2.625 in.) times its thickness (.5 in.). Each pressure tap is then assumed to act over a projected area of .4375 in^2. Since the jet is supersonic, the pressures which it exerts on the inner surface of the control should be nearly independent of the ambient pressure in the test chamber. Hence the results as given here reflect the fact that the pressure on the interior of the control extension is approximately proportional to the upstream pressure in the jet.

Net Control Force and Moment

The net effect of extending the control surface out from the base of the model is a force and moment obtained by adding (with appropriate sign) $C_{N_I} + C_{N_o} = C_{N_c}$ and $C_{m_I} + C_{m_o} = C_{m_c}$. Normal force is positive upward, and pitching moment is positive nose up.

RESULTS

Force Data

Measured normal force, axial force and pitching moment are shown as functions of angle of attack in Figure 9. These plots are obtained directly from the force balance data and include the forces due to pressures acting on the interior surfaces of the control extensions. Each control segment increases the normal force coefficient on the body by about .02.

Control Effectiveness

Plots of control functions are shown in Figures 10 and 11. The net normal force (Figure 10), for example, is determined by subtracting the body alone data from the body plus control (corrected for the pressures acting on the interior of the control surface in the wind tunnel tests). Then the downward load due to the exhaust impinging on the inside of the control surface is subtracted. The normal force data thus shows increasing downward load as the jet pressure increases and as the control extension becomes longer.

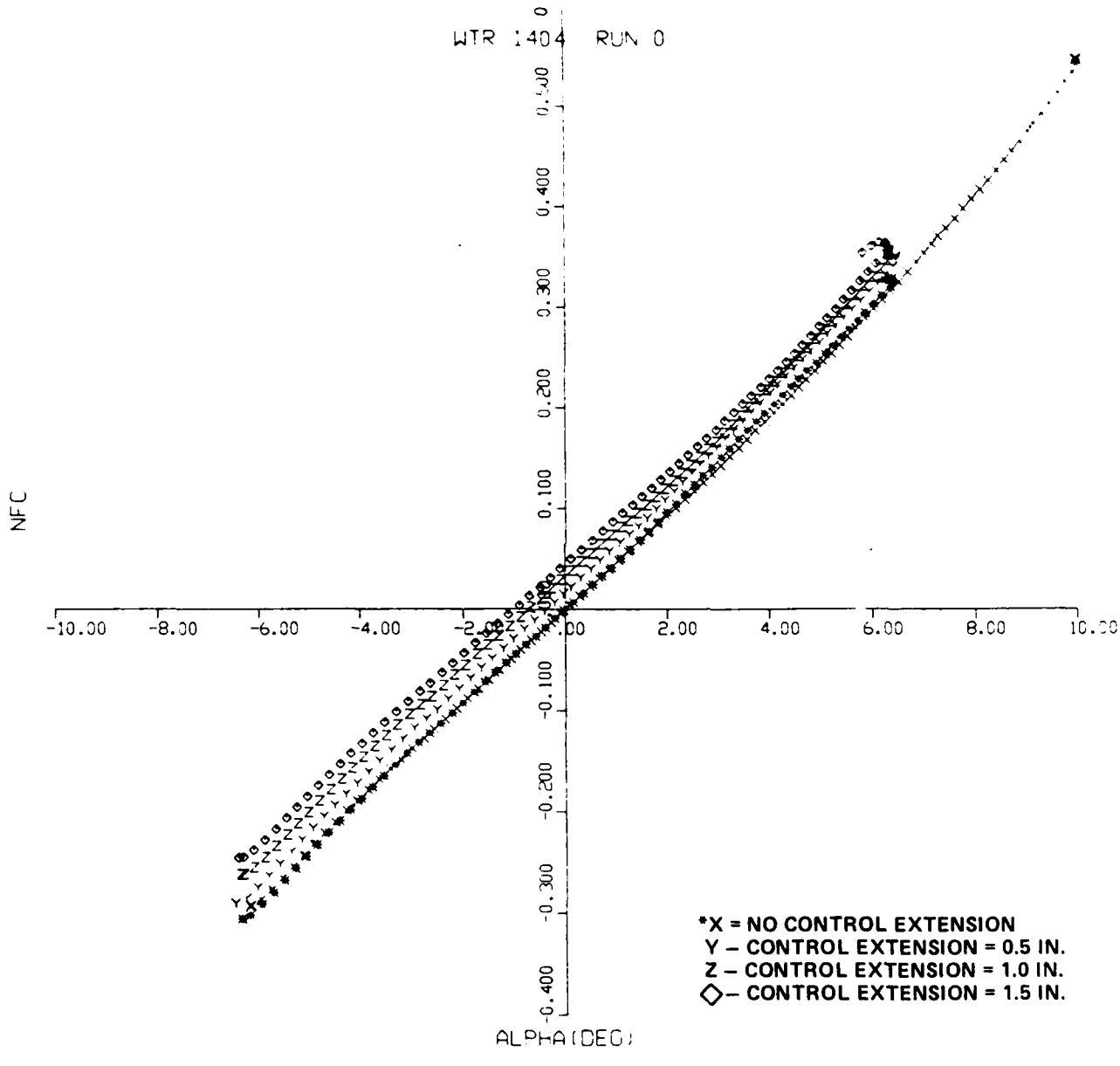

FIGURE 9a. NORMAL FORCE COEFFICIENTS

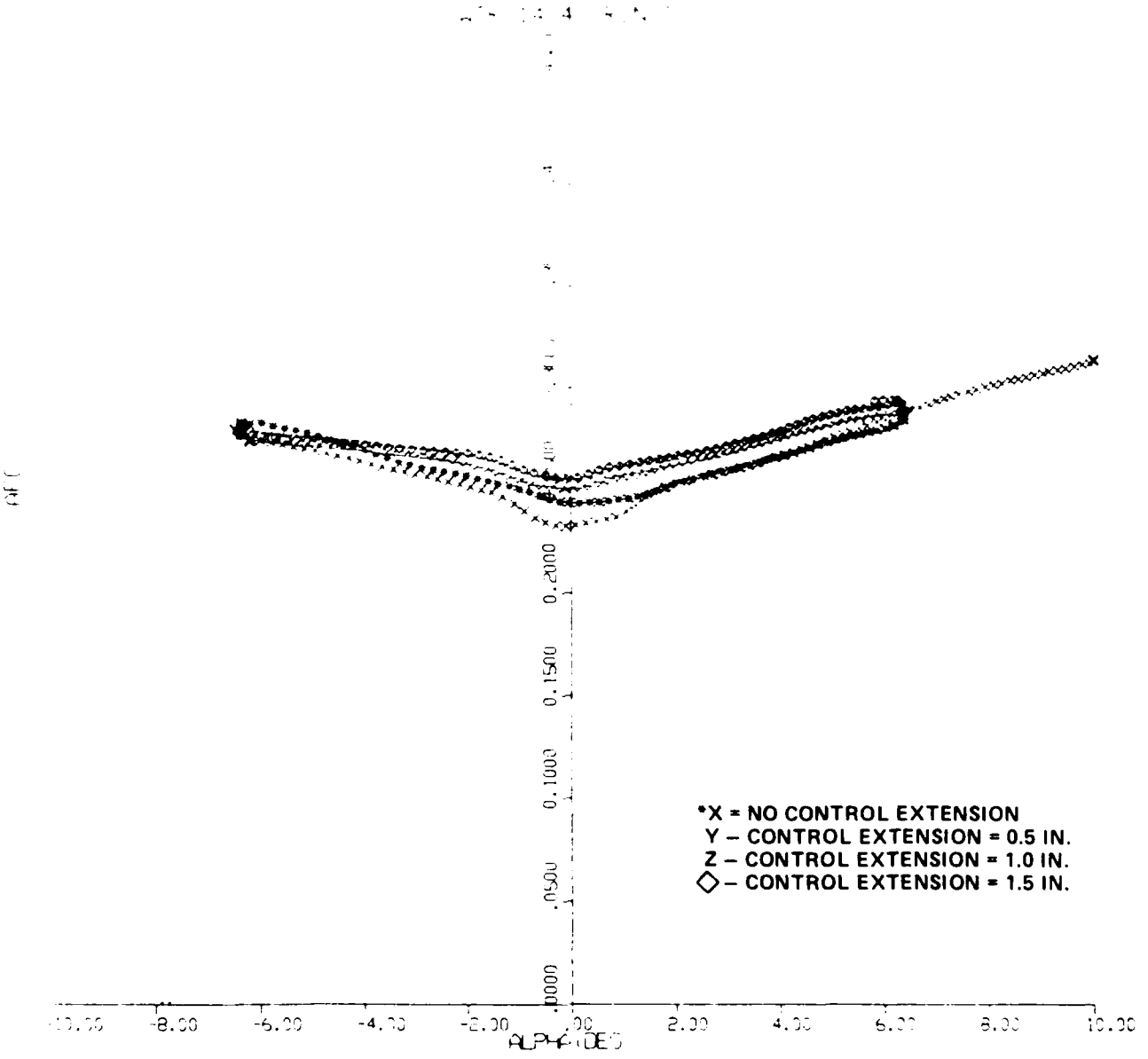

FIGURE 9b. AXIAL FORCE COEFFICIENTS

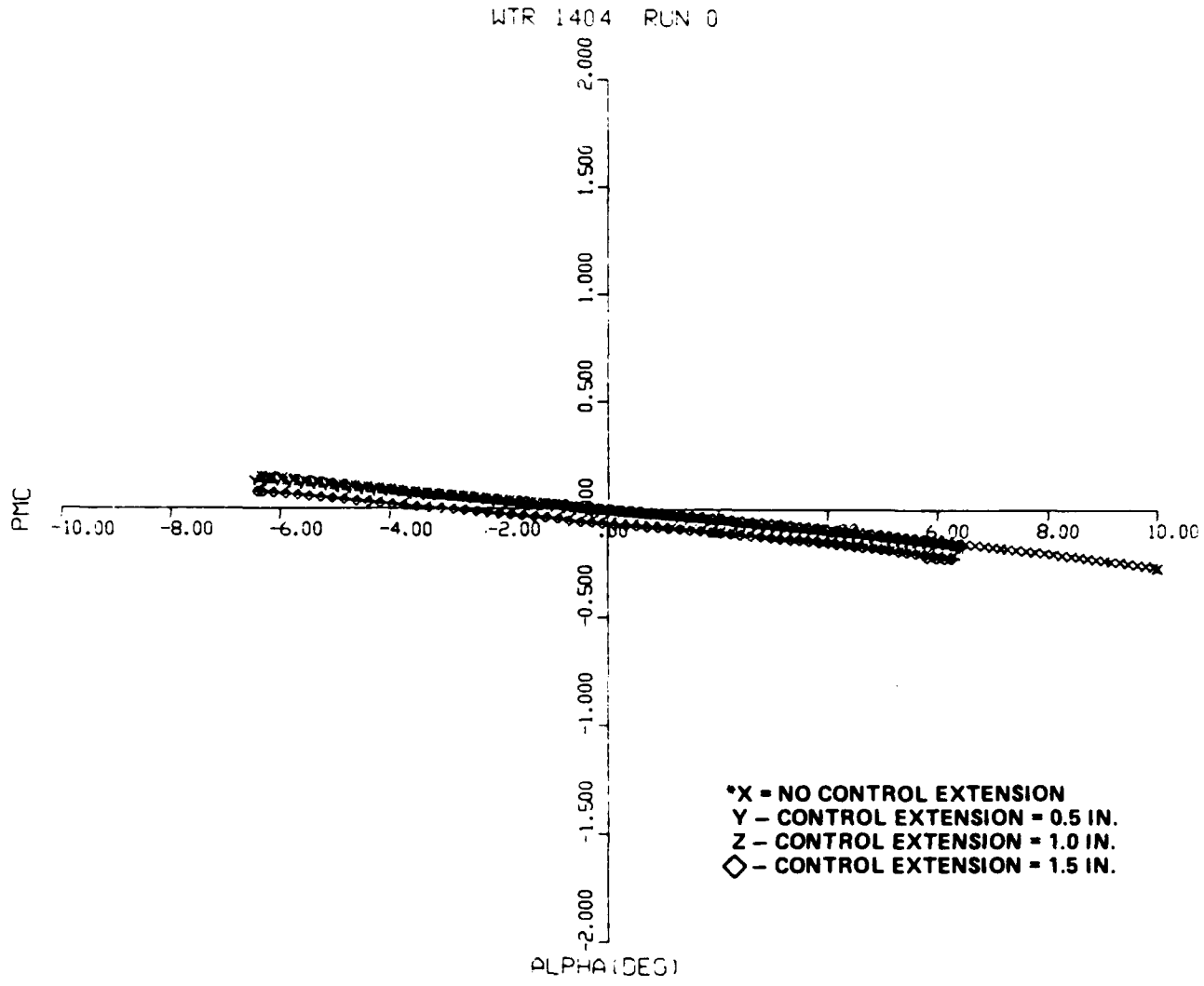

FIGURE 9c. PITCHING MOMENT COEFFICIENT

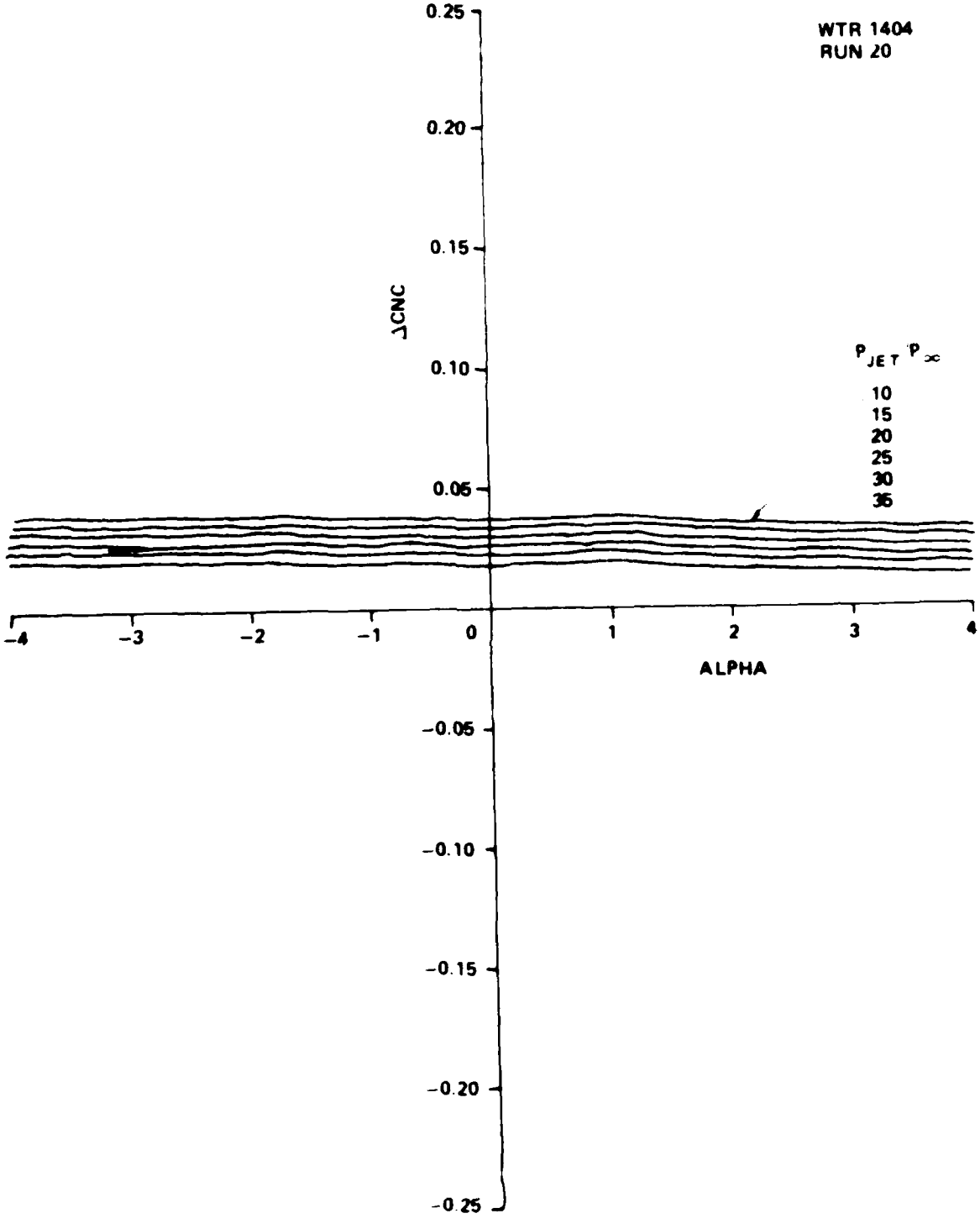

FIGURE 10a. NORMAL FORCE COEFFICIENT ON CONTROL EXTENSION OF 0.5 IN

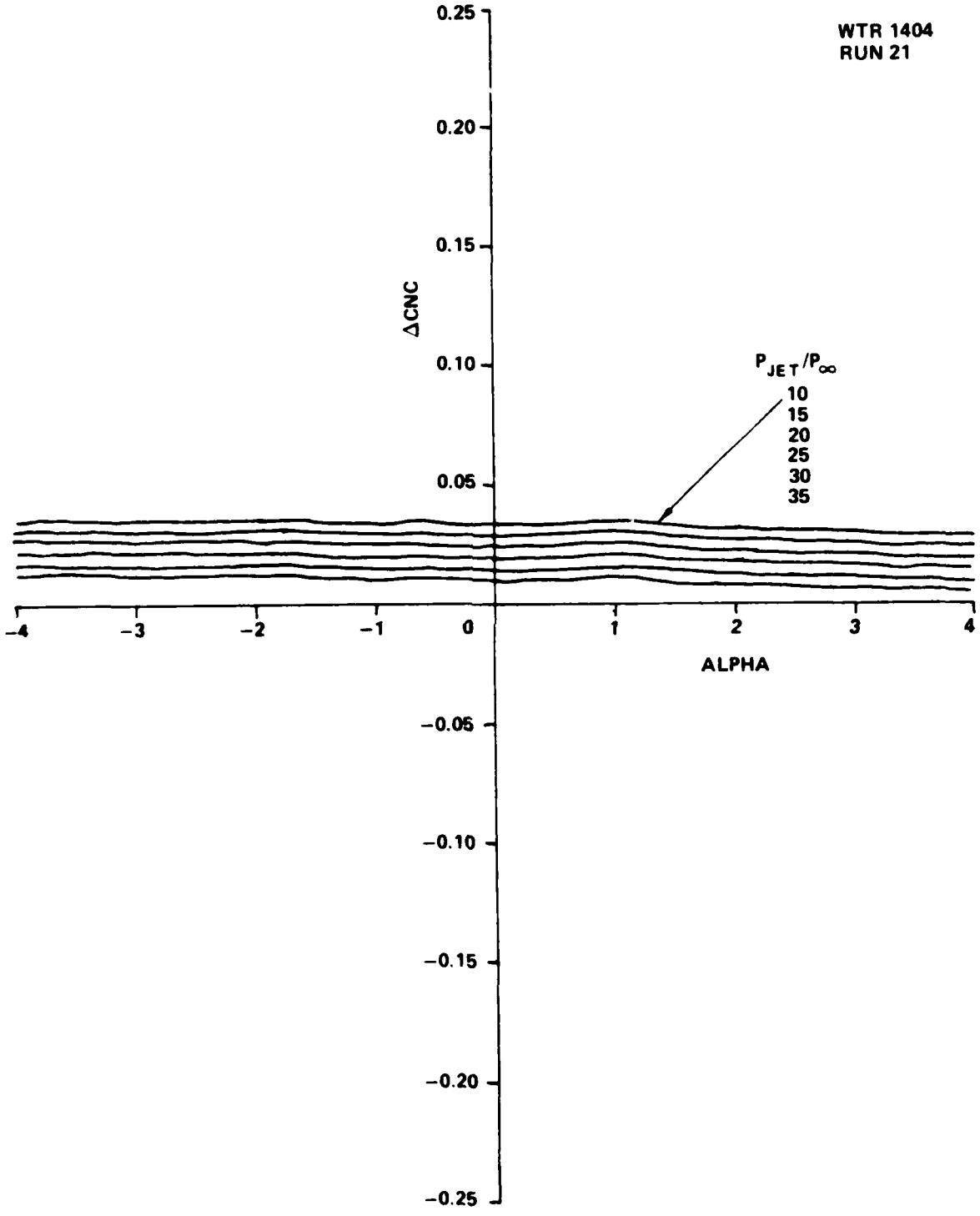

FIGURE 10a. (CONT.) NORMAL FORCE COEFFICIENT ON CONTROL EXTENSION OF 0.5 IN.

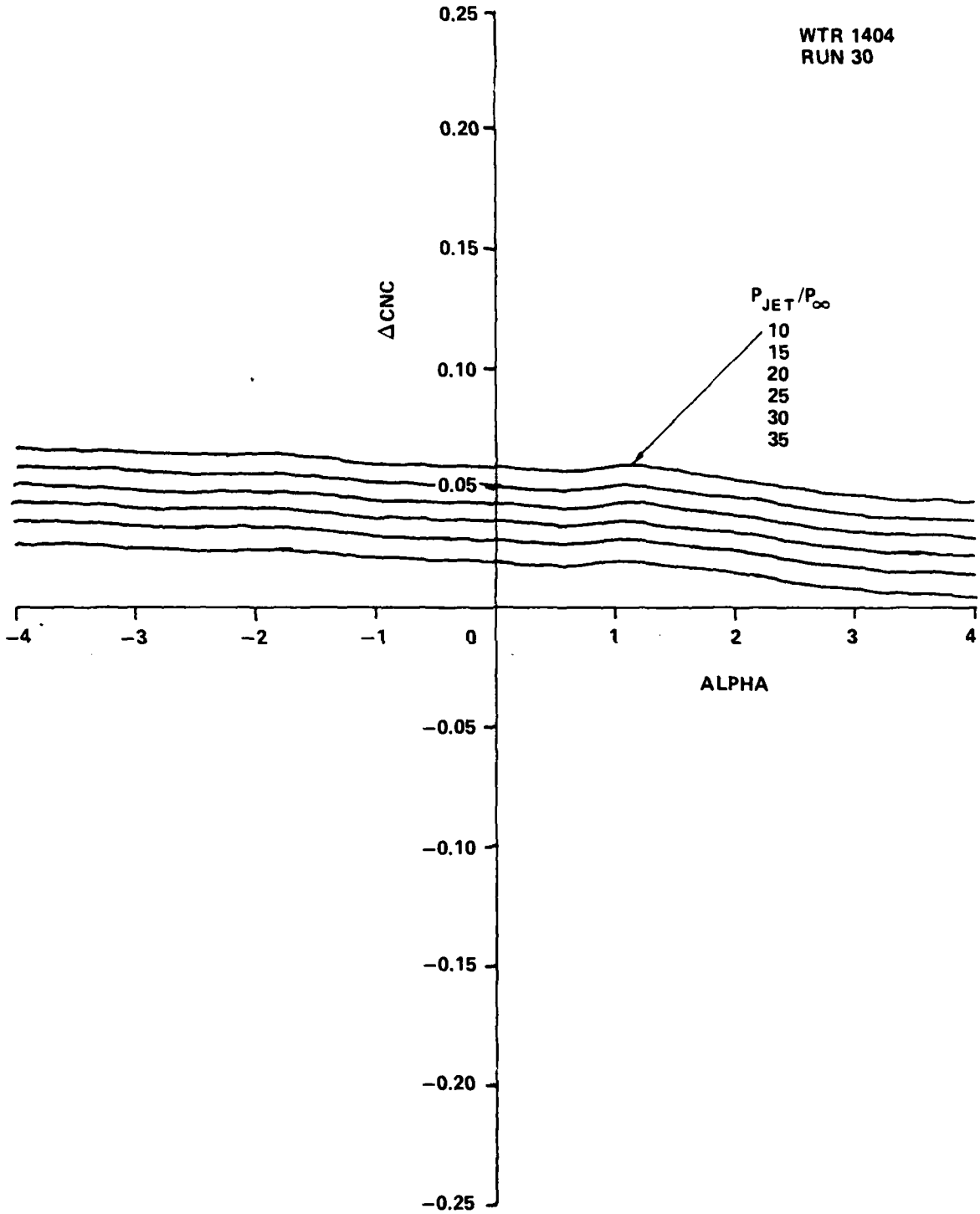

FIGURE 10b. NORMAL FORCE COEFFICIENT ON CONTROL EXTENSION OF 1 IN.

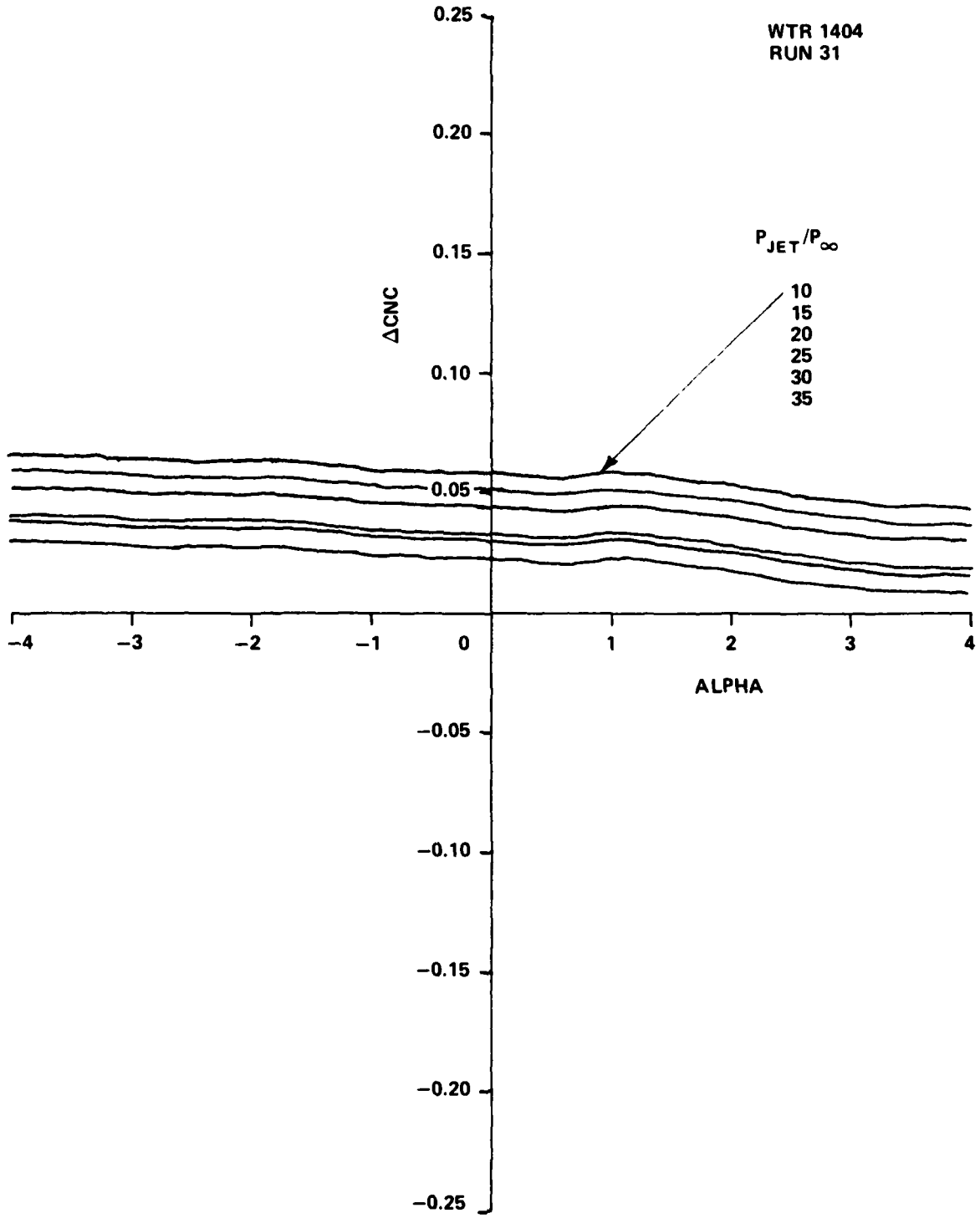

FIGURE 10b. (CONT.) NORMAL FORCE COEFFICIENT ON CONTROL EXTENSION OF 1 IN.

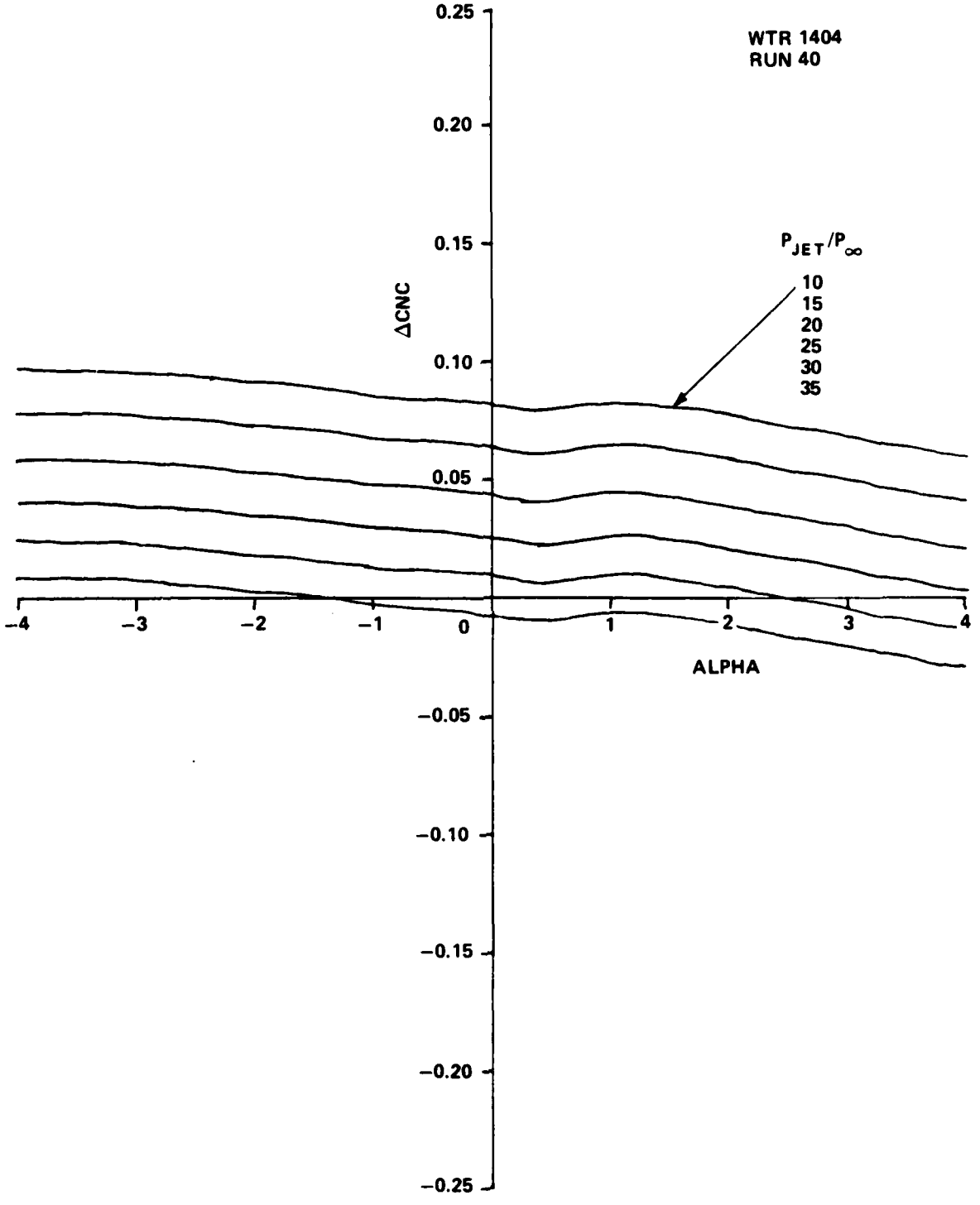

FIGURE 10c. NORMAL FORCE COEFFICIENT ON CONTROL EXTENSION OF 1.5 IN.

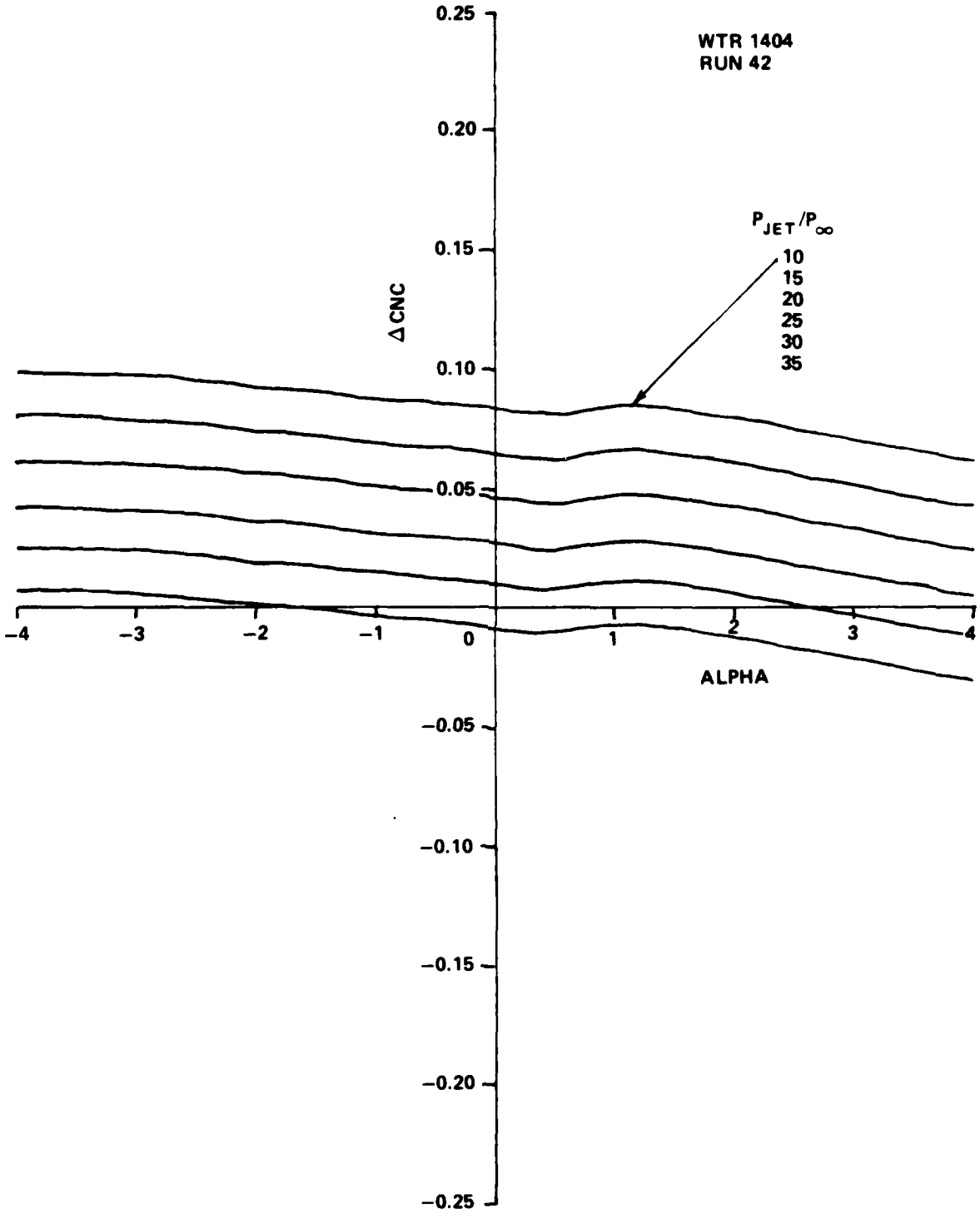

FIGURE 10c. (CONT.) NORMAL FORCE COEFFICIENT ON CONTROL EXTENSION OF 1.5 IN.

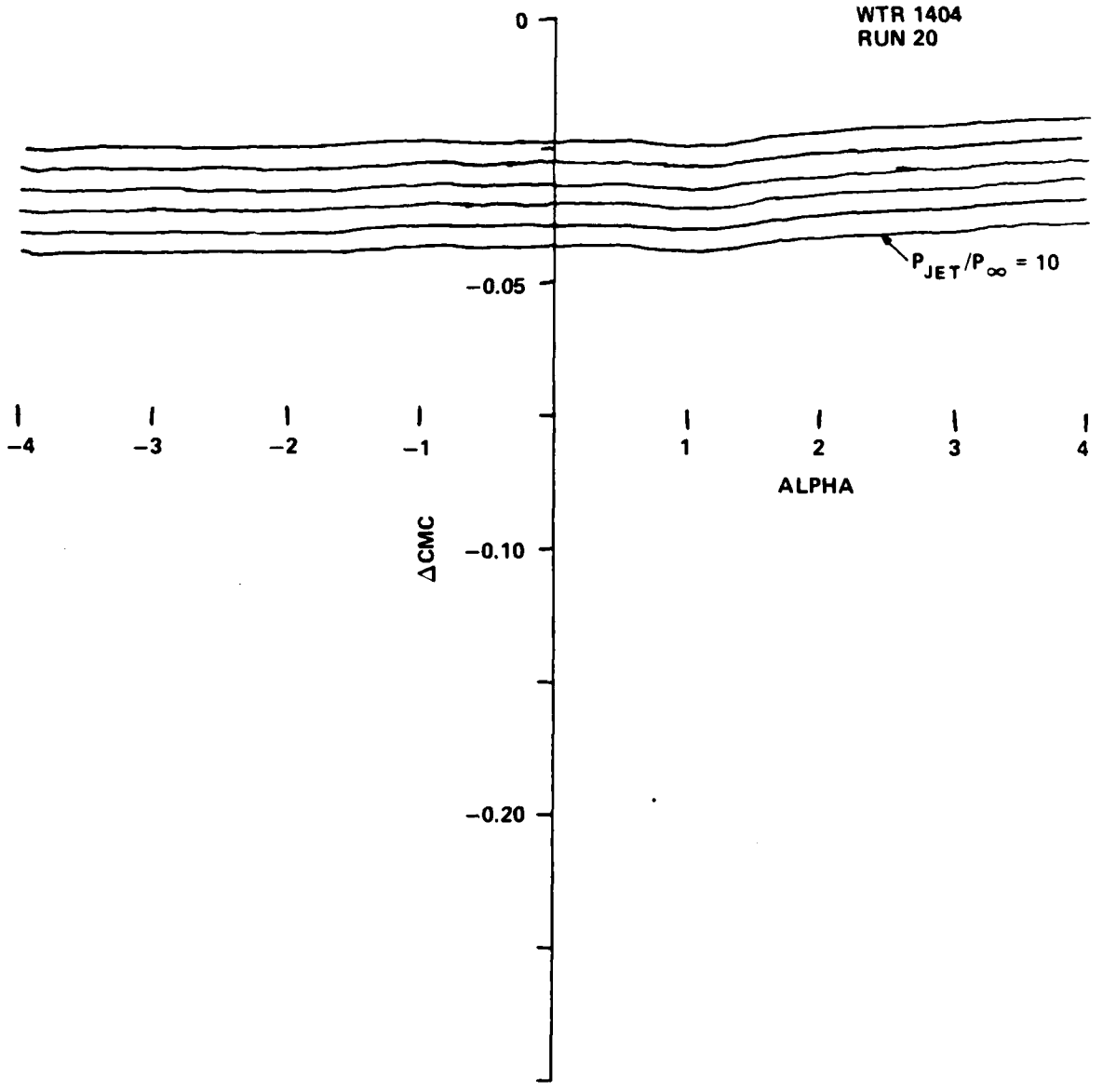

FIGURE 11a. PITCHING MOMENT COEFFICIENT DUE TO CONTROL EXTENSION OF 0.5 IN.

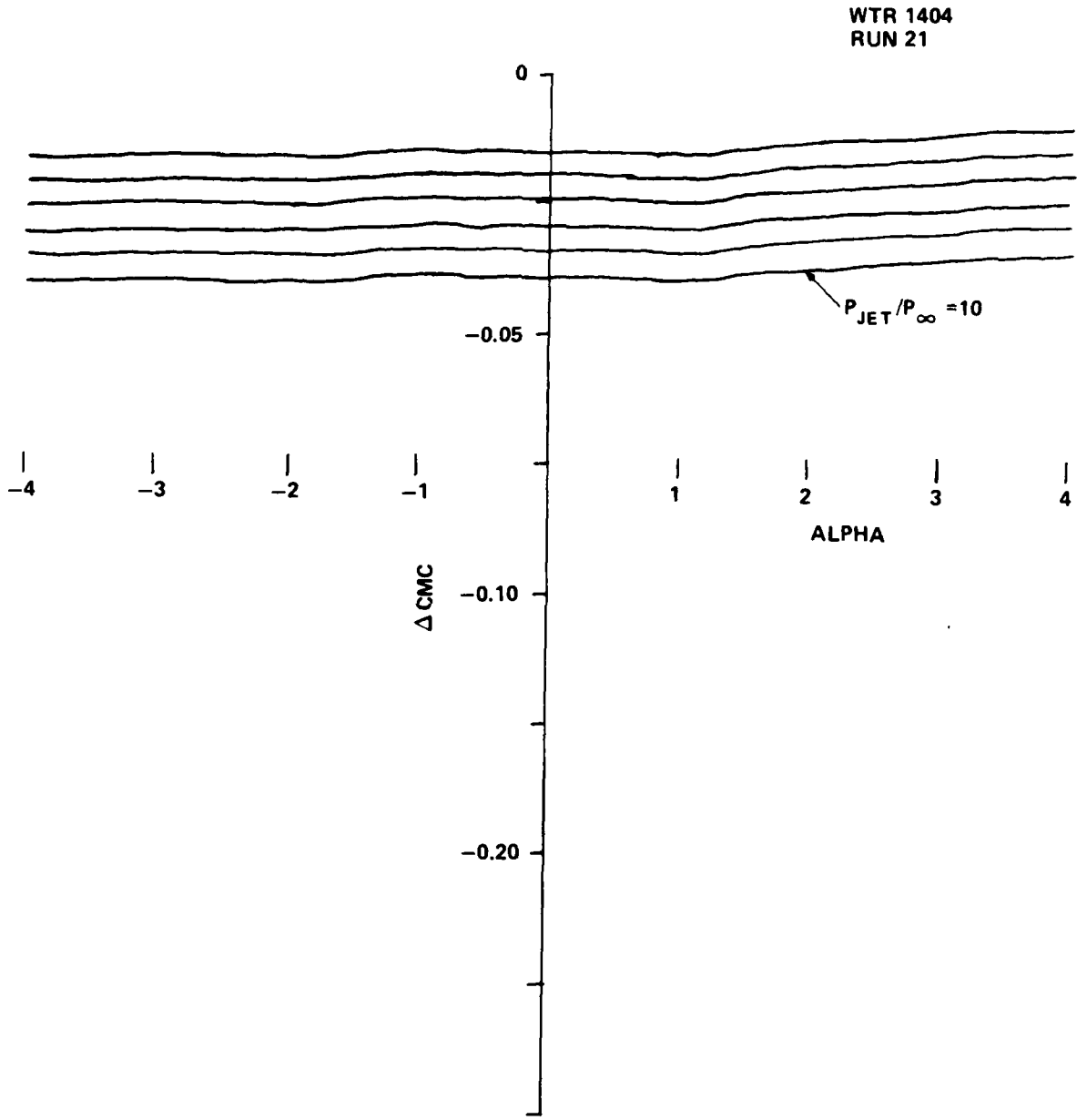

FIGURE 11a. (CONT.) PITCHING MOMENT COEFFICIENT DUE TO CONTROL EXTENSION OF 0.5 IN.

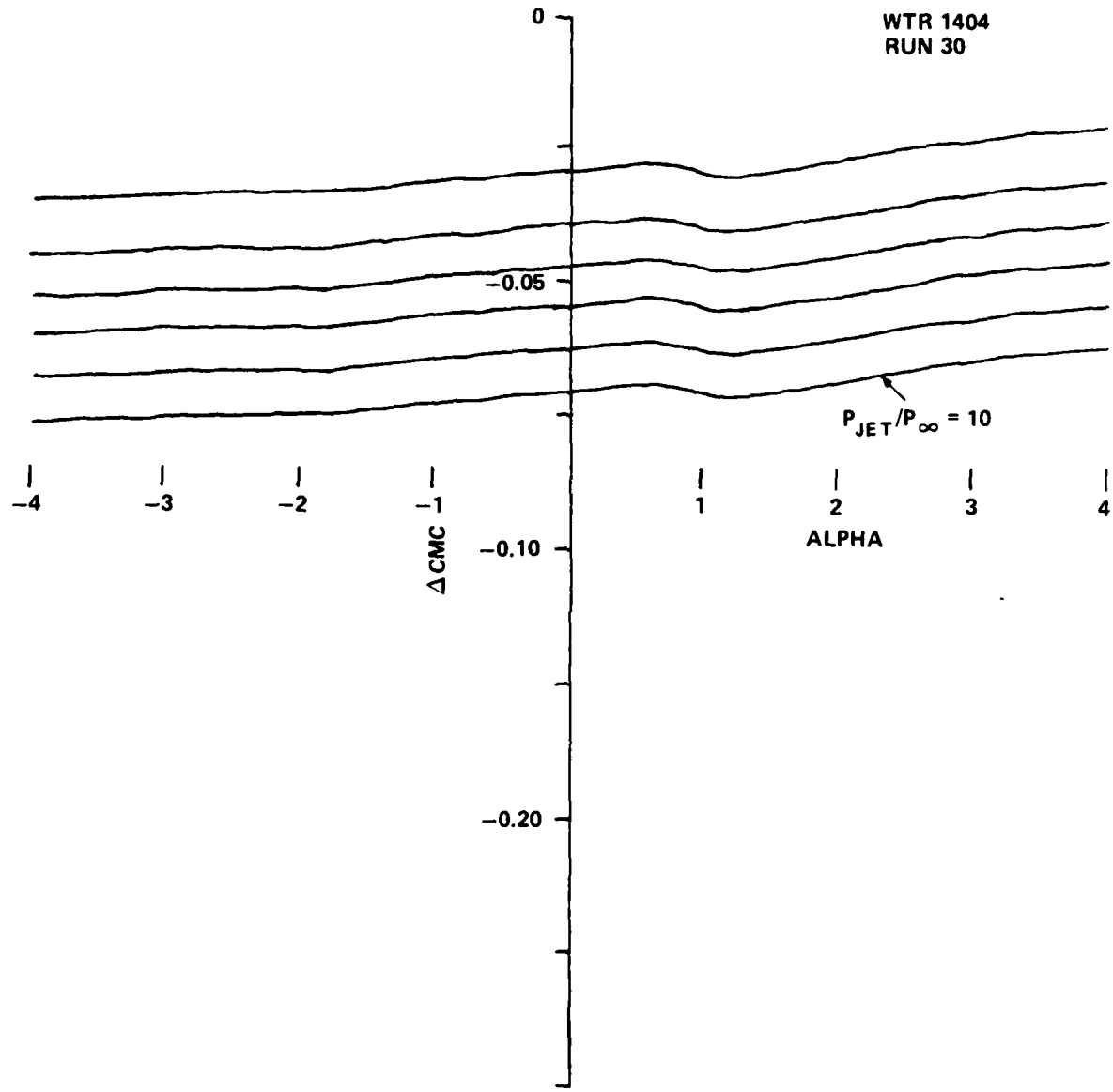

FIGURE 11b. PITCHING MOMENT COEFFICIENT DUE TO CONTROL EXTENSION OF 1 IN.

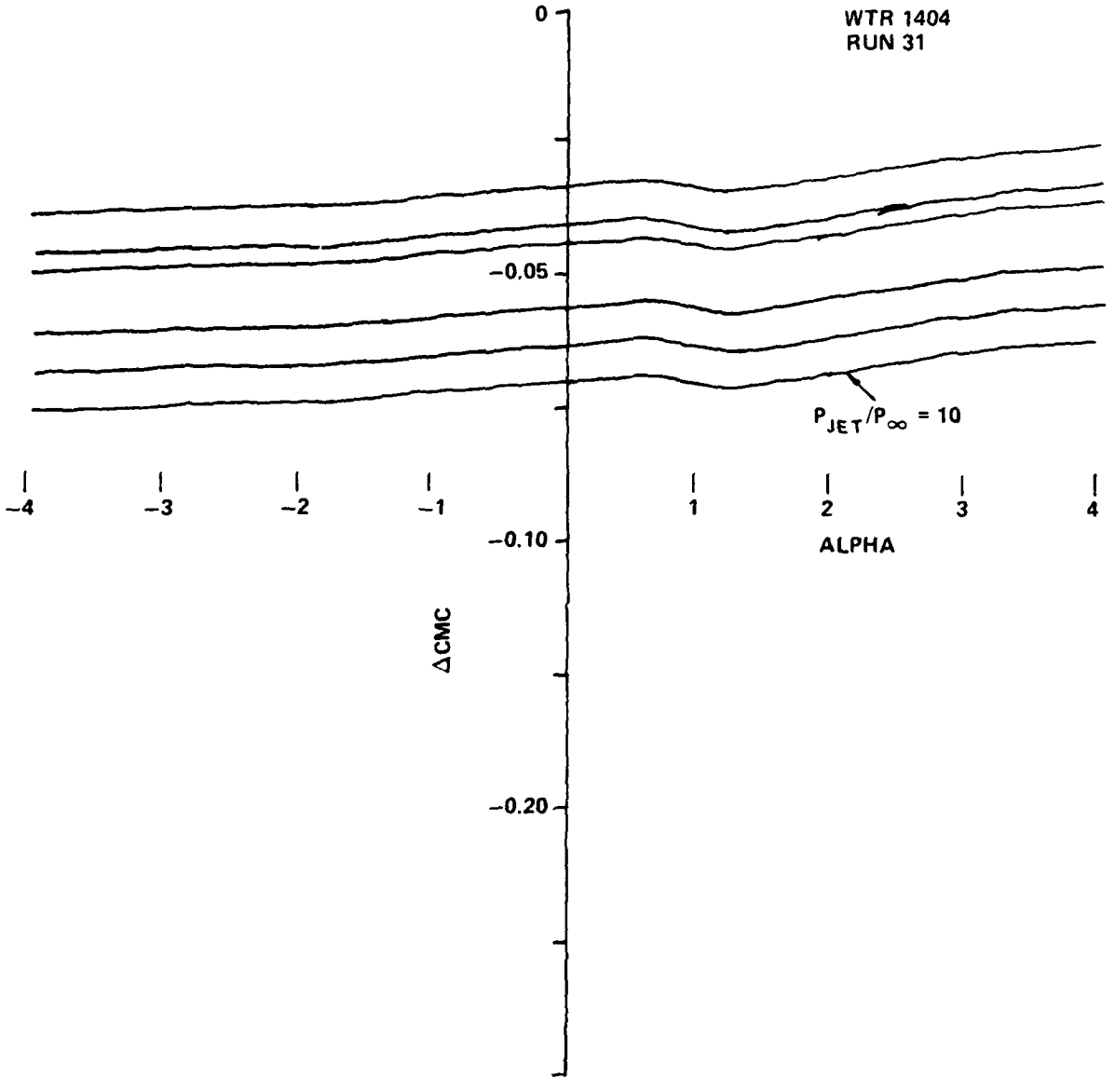

FIGURE 11b. (CONT.) PITCHING MOMENT COEFFICIENT DUE TO CONTROL EXTENSION OF 1 IN.

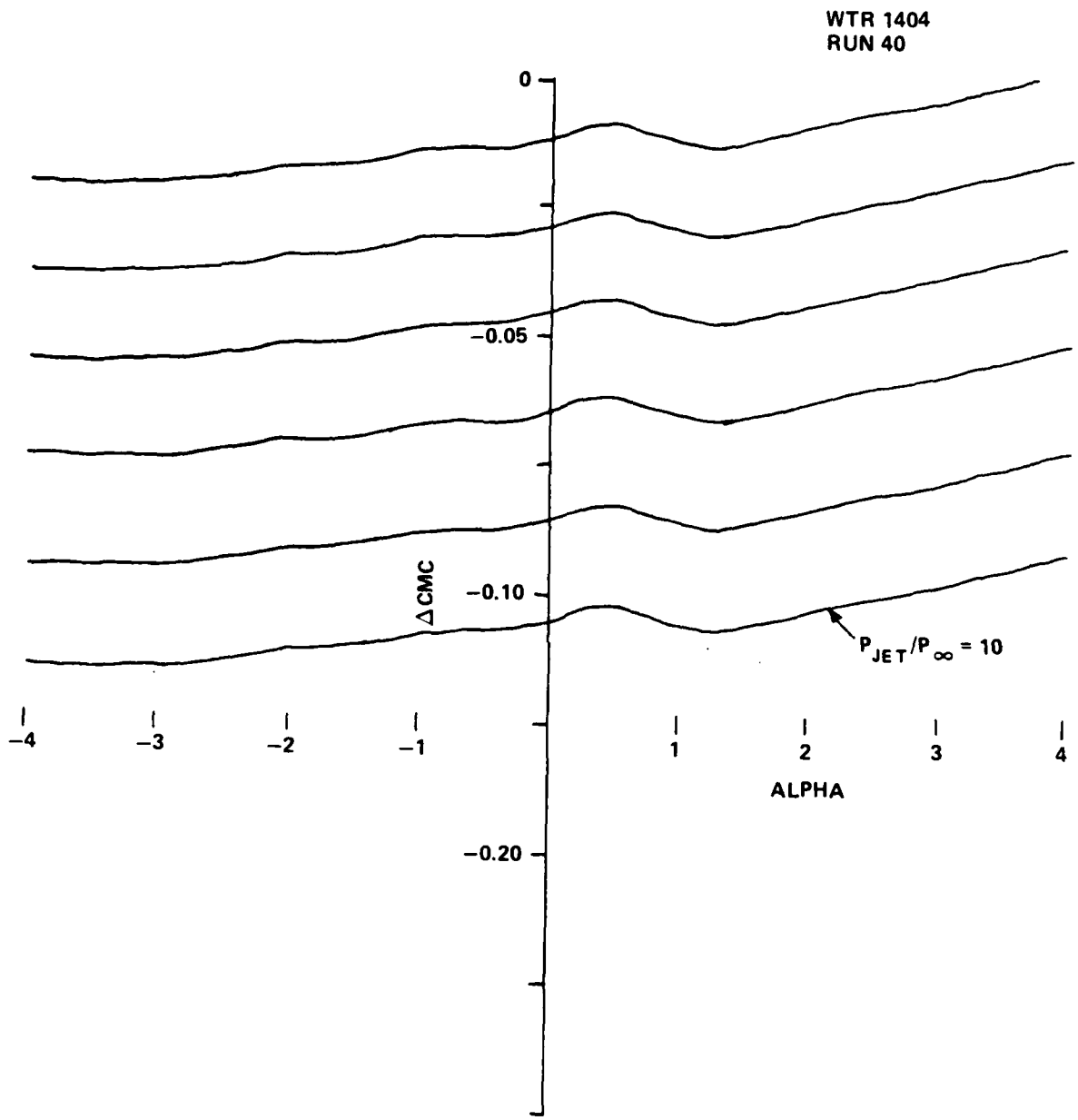

FIGURE 11c. PITCHING MOMENT COEFFICIENT DUE TO CONTROL EXTENSION OF 1.5 IN.

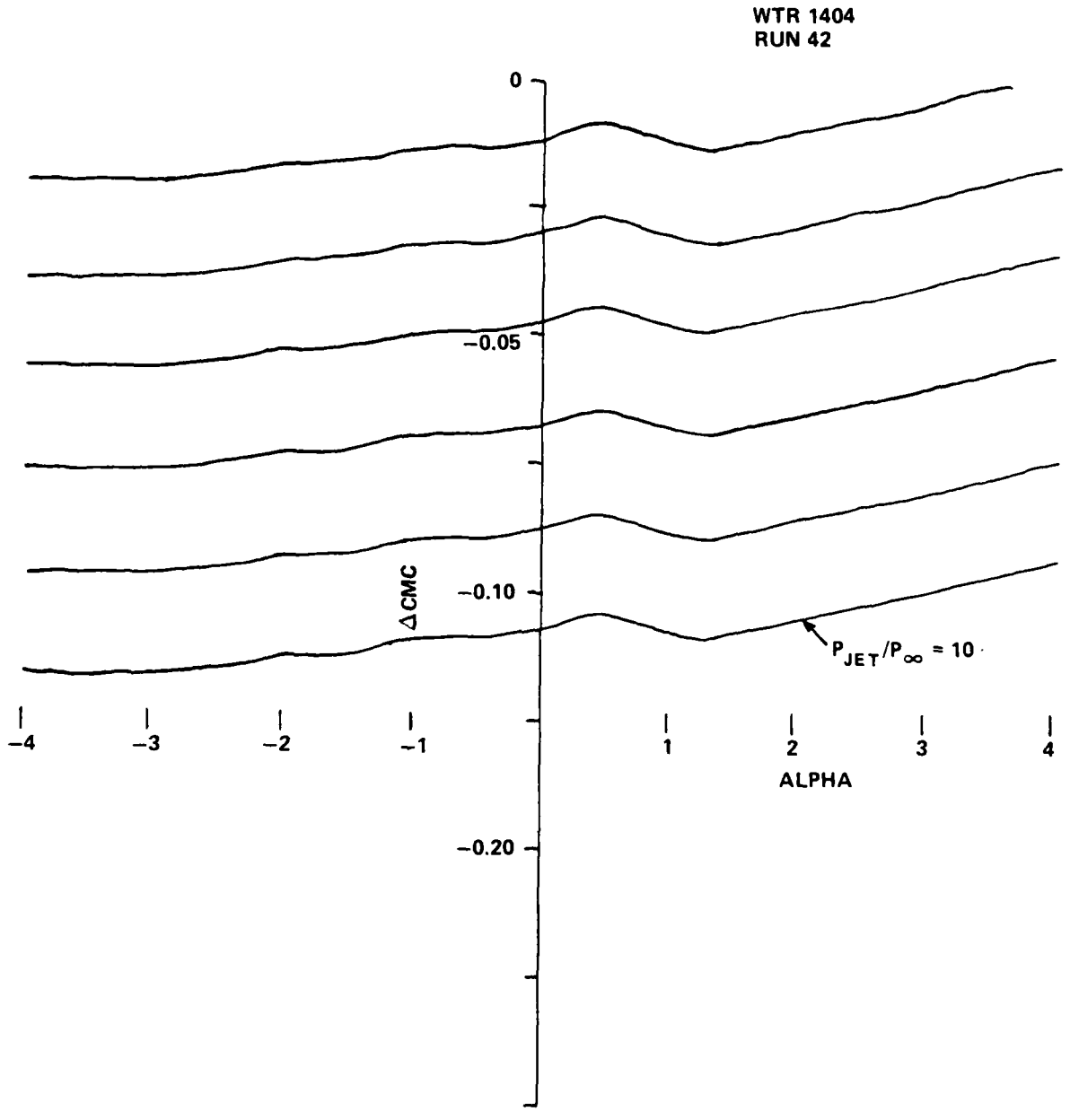

FIGURE 11c. (CONT.) PITCHING MOMENT COEFFICIENT DUE TO CONTROL EXTENSION OF 1.5 IN.

Pitching moment curves (Figure 11) show similar trends.

The effectiveness provided by the sliding control system is more explicitly shown in Figures 12 and 13. Here the control forces and moments are plotted against control extension for different jet pressure ratios. Although the plots apply at zero angle of attack, the results at other angles of attack would be similar. At a pressure ratio of about 150, the jet would be correctly expanded in this example.

In the experimental setup for the interior pressures on the control extensions, air at a high upstream pressure (about 60 psi) was expanded into a near-vacuum; the jet was therefore underexpanded during the tests. However, the pressure exerted on the control surface was generally lower than the ambient pressure on the model during the force test, and also lower than the pressure acting on the outside of the control extensions. Consequently, as can be seen in Figures 12 and 13, for low jet pressure ratios (p_{JET}/ρ_∞ = 10, for example), or for engine-off the control extensions carry a net upward force that increases as the extension gets longer. At high jet pressures (p_{JET}/ρ_∞ = 35), the net force on the control extension is still primarily upward, but the force decreases as the control extends beyond about 1 in. and acts downward at a control extension of 1.5 in. The pressures measured on the interior surfaces of the control extensions in the presence of the jet were slightly higher near the body than on the outboard extension. Hence the pitching moment was still negative when the control force changed sign.

SCHLIEREN PICTURES

Schlieren photographs of the model in the wind tunnel are shown in Figure 14. The flow at the base of the model appears to be relatively unaffected by the model support system.

The jet flow patterns are visible in the pictures shown in Figure 15. In the case with no control extension, the jet is symmetrical; while the addition of the control section apparently causes an upward deflection of the flow in the vicinity of the control.

ACCURACY

Force and pressure data are quite repeatable and accurate (within a few percent) although differences of up to 20 percent sometimes appeared between supposedly symmetric pressure readings. Probably, the main source of error is the paucity of pressure data so that integrated forces on the interior surfaces of the control extension could be off by 10 percent or more. The results should be sufficiently accurate, however, to indicate the general effectiveness of the concept

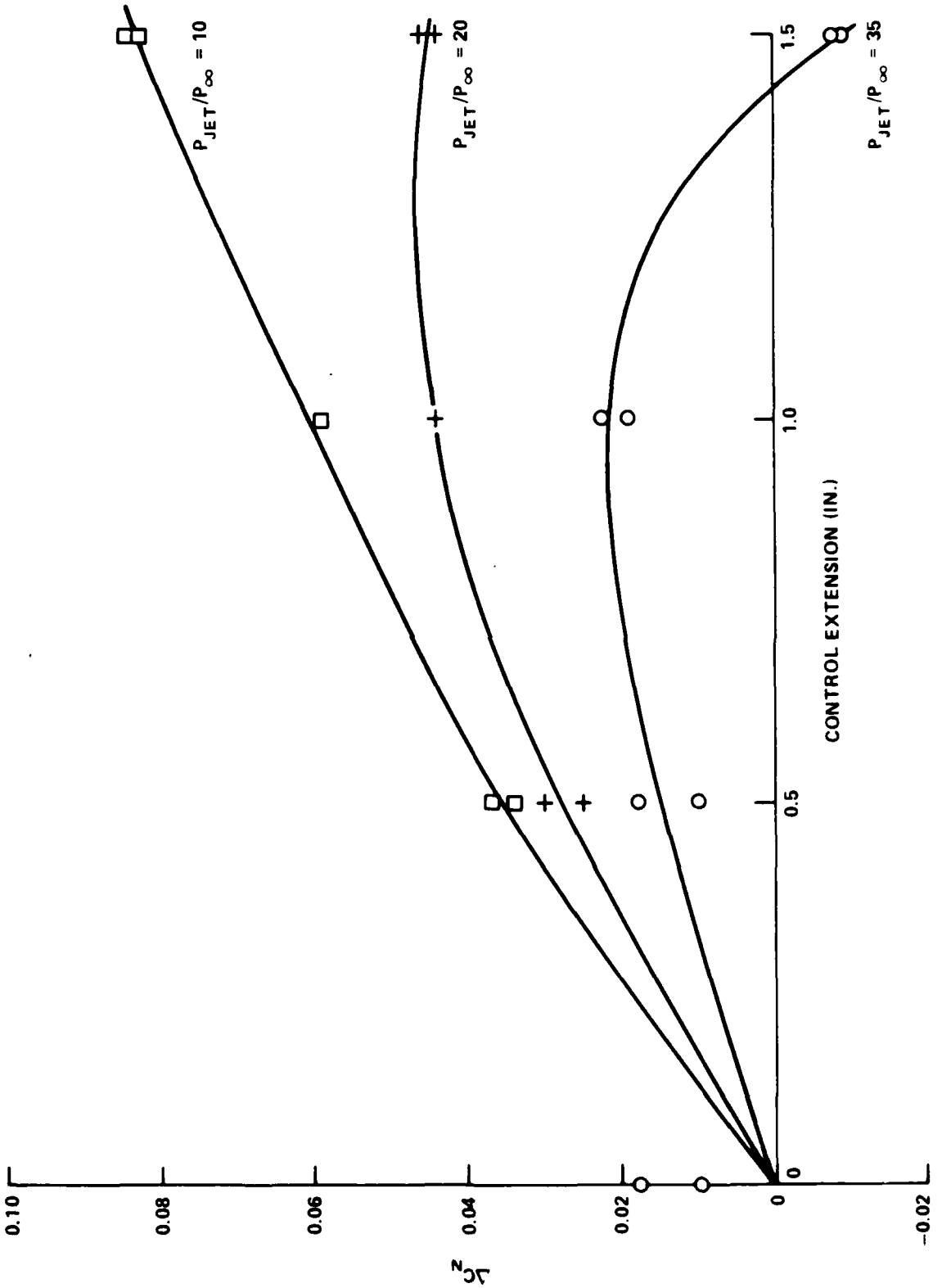

FIGURE 12. CONTROL FORCE COEFFICIENT AT $\alpha = 0°$

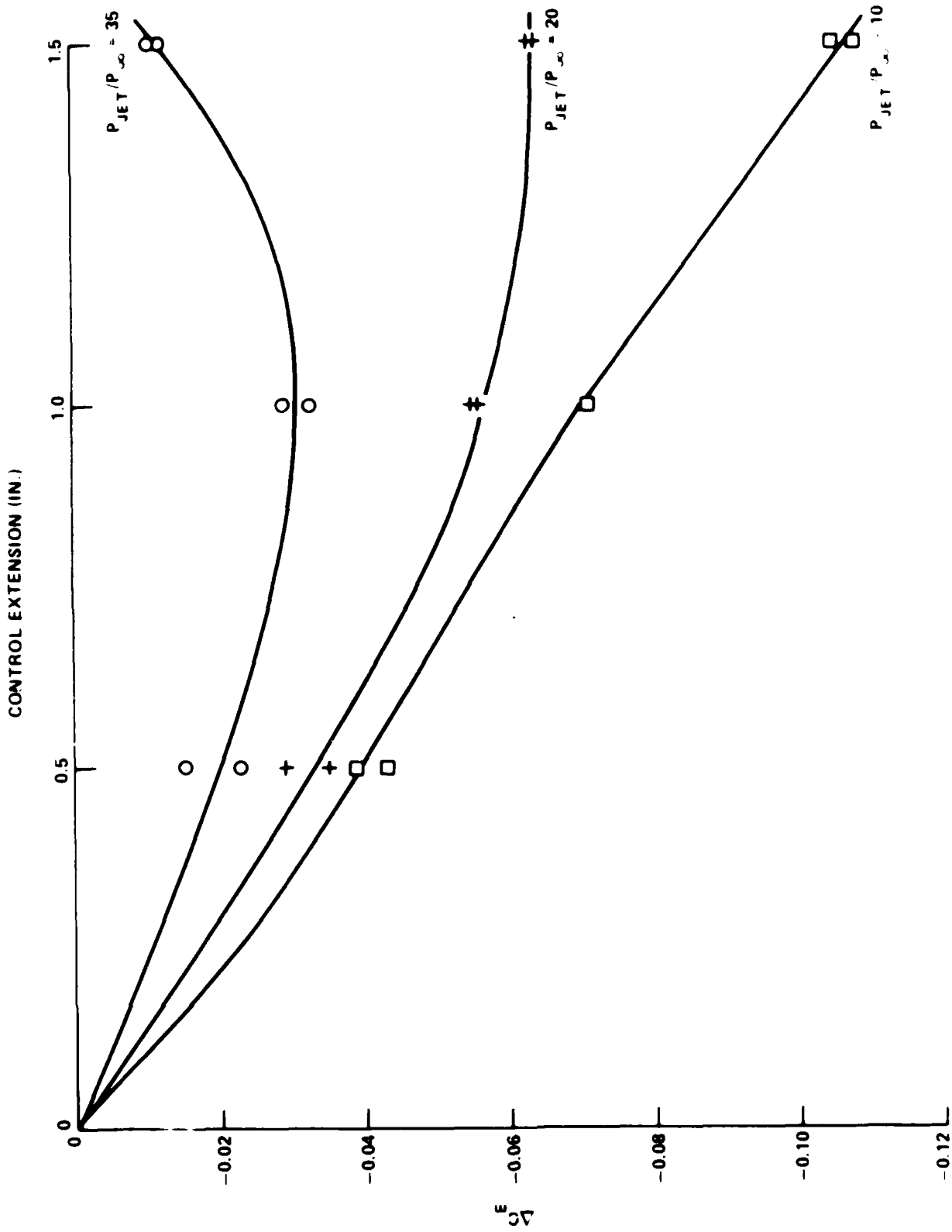

FIGURE 13. CONTROL PITCHING MOMENT COEFFICIENT AT $\alpha = 0°$

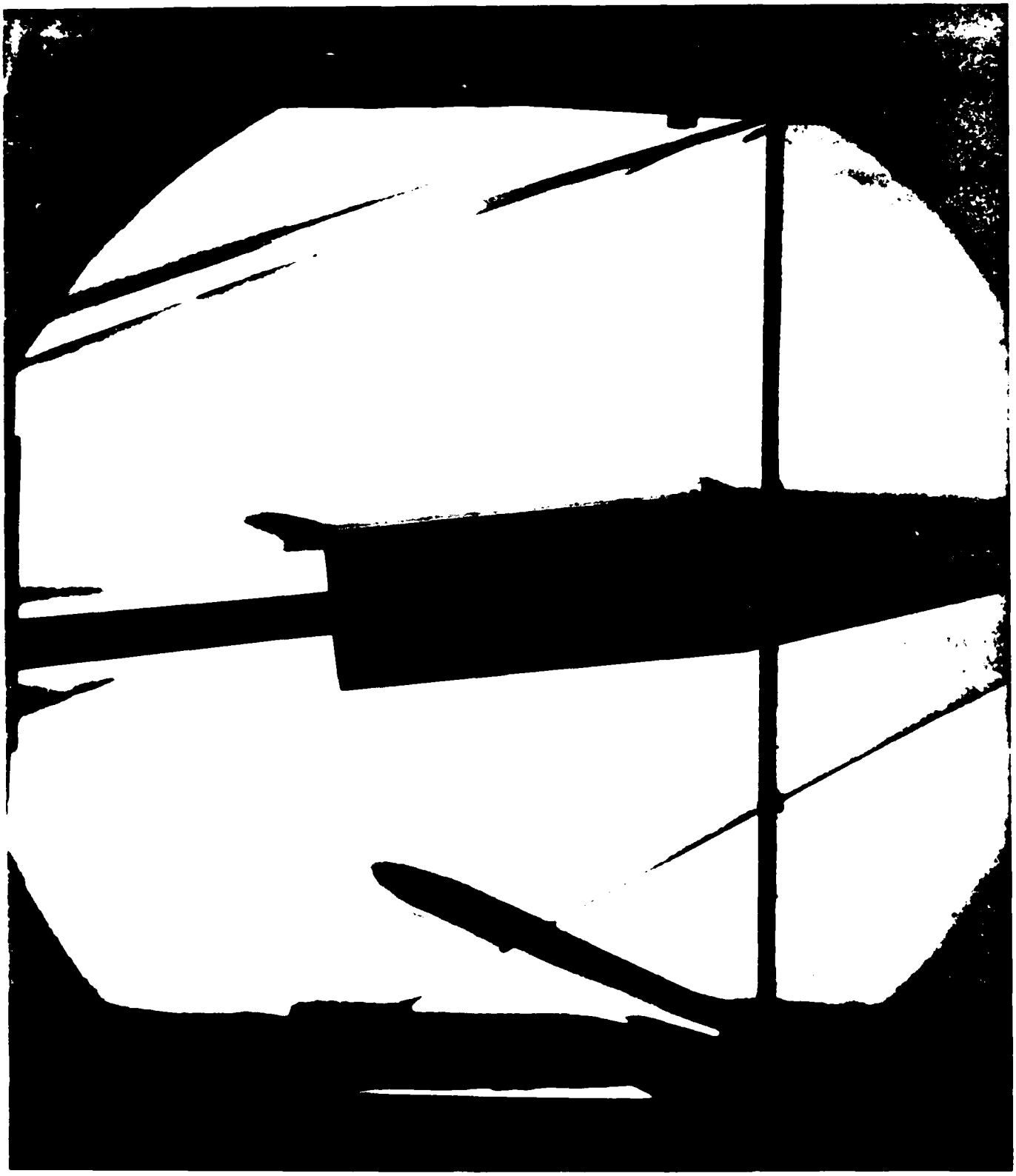

FIGURE 14a SCHLIEREN PHOTOGRAPHS OF MODELS AT 4° ANGLE OF ATTACK. NO CONTROL EXTENSION

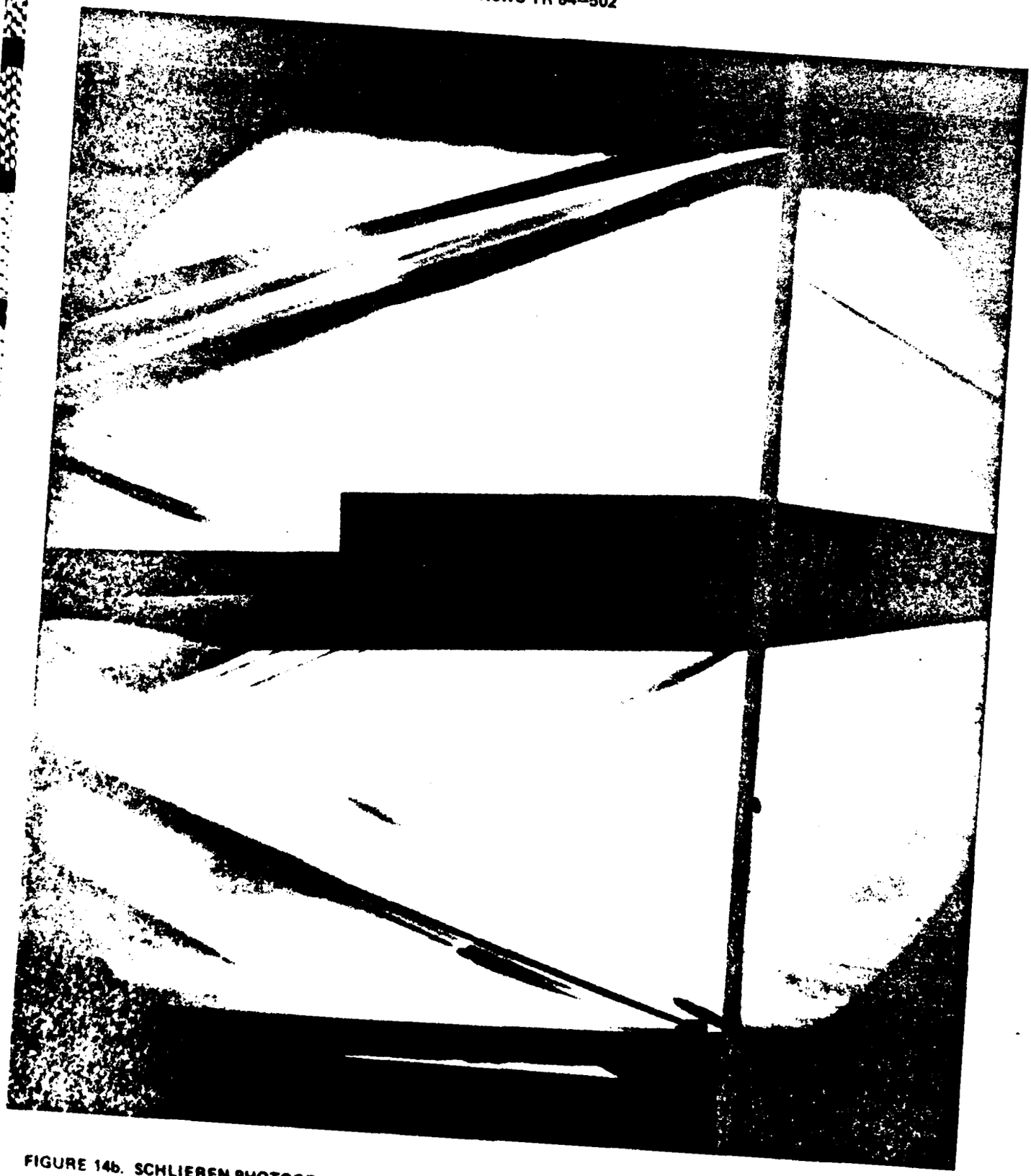

FIGURE 14b. SCHLIEREN PHOTOGRAPHS OF MODELS AT 4° ANGLE OF ATTACK. CONTROL EXTENSION = 1.5 IN.

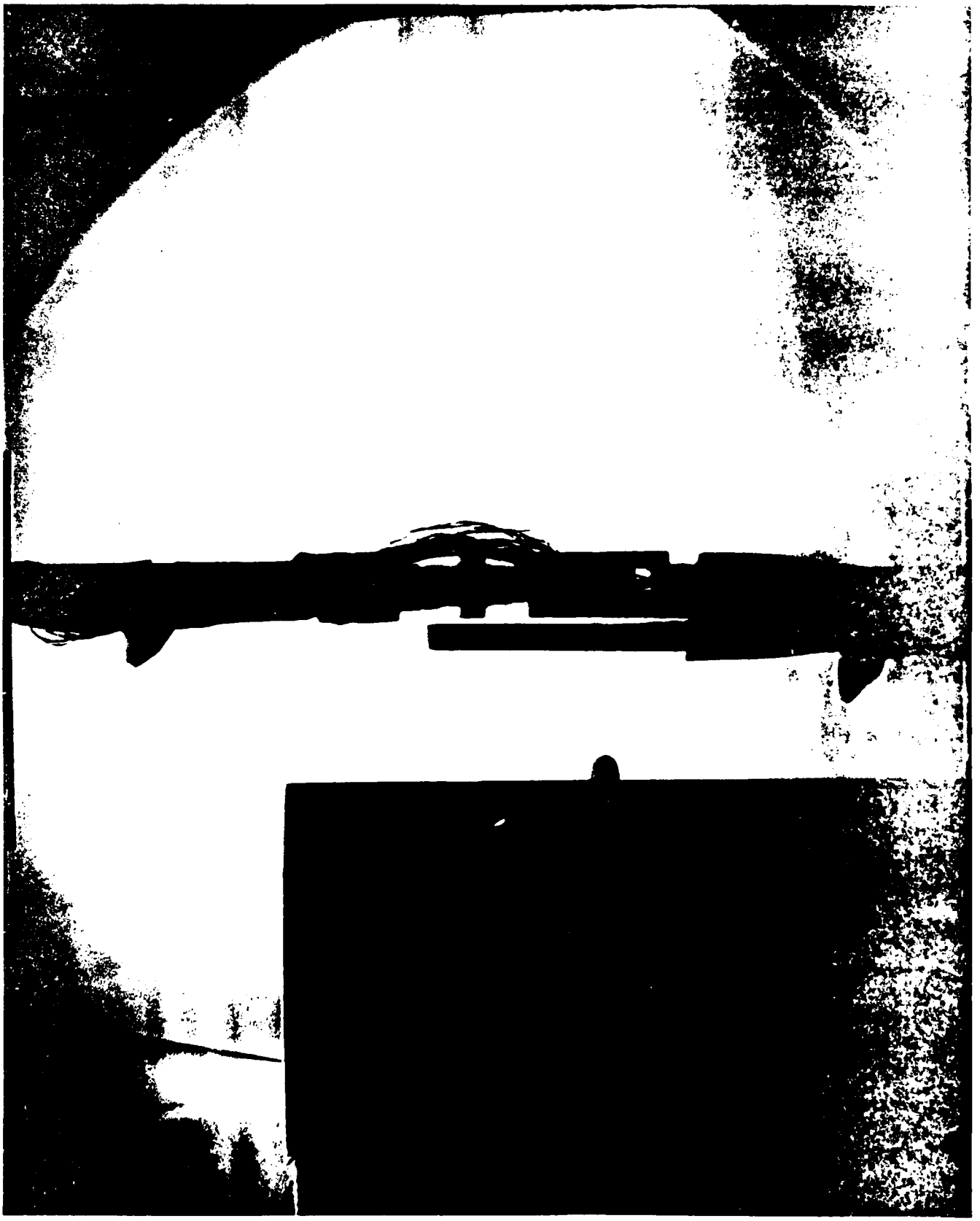

FIGURE 15a. SCHLIEREN PHOTOGRAPHS OF JET. NO CONTROL EXTENSION

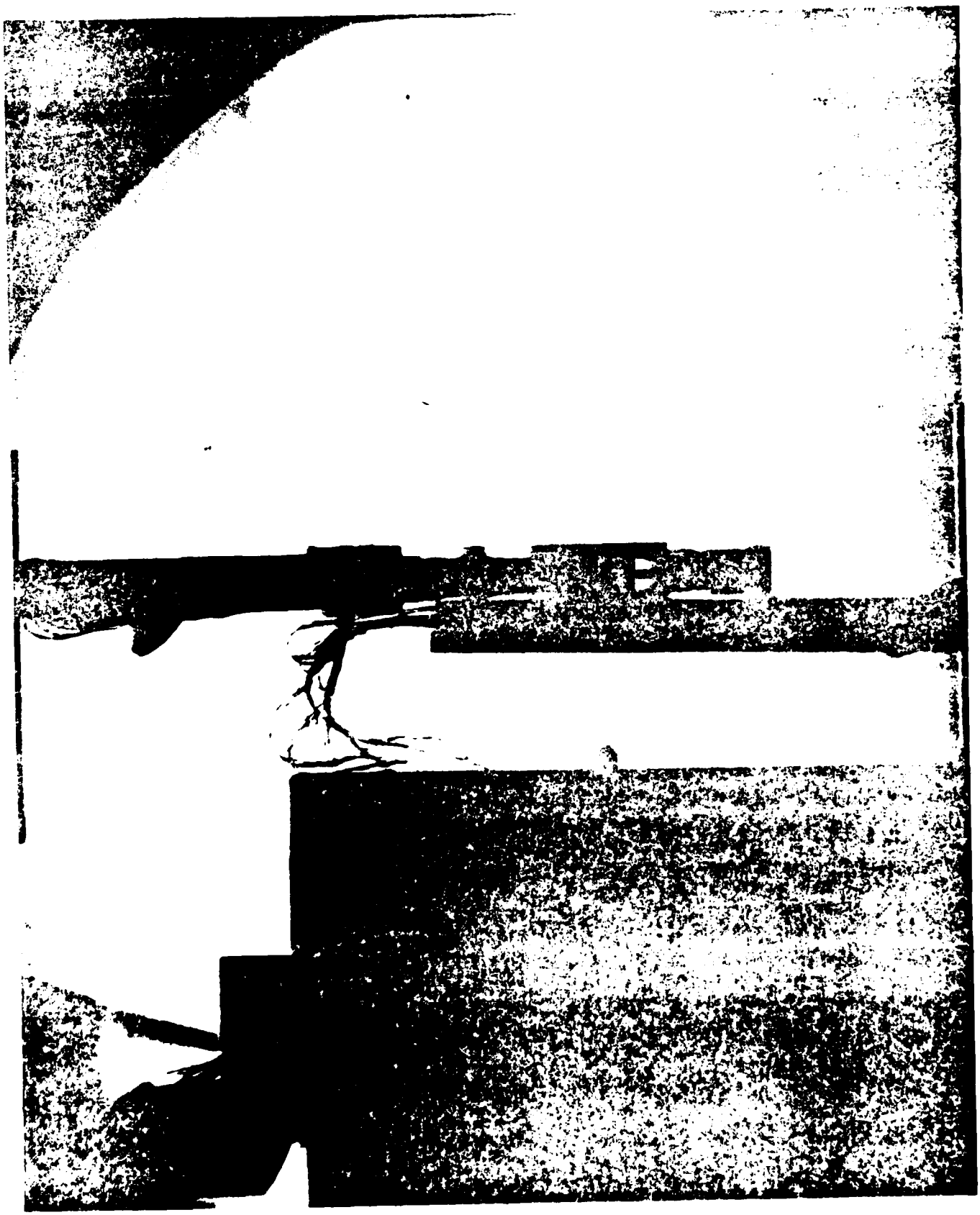

FIGURE 15b. SCHLIEREN PHOTOGRAPHS OF JET. CONTROL EXTENSION = 1 IN.

CHAPTER 5

CONCLUSIONS

The results of the experiment indicate that a sliding surface can be an efficient and effective control device. The measurements shown here for jet pressure ratios less than 10 or 15 indicated that the concept could provide trim moments for engine-off or low thrust conditions.

Scaling the pressure on the interior of the control surface with jet pressure ratio would indicate that for ratios in excess of about 55, the pressure on the inside of the control would exceed the pressure on the outside, and the device could then provide trim or control moments of the opposite sign from engine-off conditions.

As indicated previously, a sliding control concept can operate at high altitude and could be designed for low drag and low actuator force requirements.

If the device is used to trim a stable symmetric missile at a positive angle of attack, then it would be placed so as to provide a positive pitching moment. In some asymmetric configurations, such as that depicted in Figure 2, a negative trimming moment might be required; in which case the control would be placed above the jet exhaust (for high jet pressure ratios).

In general, while the control surface will generate some force after rocket engine burn-out, the direction of the force is likely to be opposite to that of the engine-on-force. Thus the system investigated here is probably not suitable for controlling both power-on and power-off flight. The situation might be different for an air-breathing engine which operates at a low pressure ratio and could continue to provide a flow field after burn-out.

It is not necessary to slide the controls in a direction parallel to the missile and thrust axis. If the control is pointed more toward the thrust axis, then it would be expected to generate a bigger interior force and more drag. Sliding the control on a line slightly away from the thrust axis would reduce the control force, but may also reduce the drag penalty for a given control moment. The optimum direction would depend on the requirements of a particular application.

Although the effect of the sliding control on the missile thrust has not been specifically investigated, it should be negligible for the case of a control sliding in the direction of the thrust axis. In a supersonic jet, there would be no upstream influence of the control. Hence only the control surface itself would experience a change of force and it would not have a streamwise component other than friction drag.

The purpose of this investigation has been to suggest a new type of control concept which might have advantages for some applications. The data presented here can provide some indication of the magnitude of the forces available for one example of this type of system; but the results can only be interpreted qualitatively for any other geometry.

DISTRIBUTION

	Copies
Commander	
Naval Sea Systems Command	
Attn: SEA 62R41 (Mr. L. Pasiuk)	1
SEA 62Z3	1
SEA 62Z31	1
SEA 62Z32	1
Technical Library	1
Washington, DC 20362	
Chief of Naval Material	
Attn: Technical Library	1
Washington, DC 20360	
Commander	
Naval Air Systems Command	
Attn: AIR-320C	1
Technical Library	1
Washington, DC 20361	
Commander	
Naval Weapons Center	
Attn: Mr. R. E. Smith	1
Mr. F. Zarlingo	1
Mr. R. Van Aken	1
Technical Library	1
China Lake, CA 93555	
Commander	
Pacific Missile Test Center	
Attn: Technical Library	1
Point Mugu, CA 93041	
Commanding General	
ARRADCOM	
Picatinny Arsenal	
Attn: Mr. A. Loeb	1
Technical Library	1
Dover, NJ 07801	

	Copies
NASA	
Attn: Technical Library	1
Washington, DC 20546	
Commander	
David W. Taylor Naval Ship	
Research and Development Center	
Attn: Mr. T. C. Tai	1
Technical Library	1
Washington, DC 20007	
Office of Naval Research	
Attn: Dr. R. Whitehead	1
Technical Library	1
800 North Quincy Street	
Arlington, VA 22217	
Commanding Officer	
Naval Air Development Center	
Attn: Technical Library	1
Warminster, PA 18974	
Superintendent	
U.S. Naval Academy	
Attn: Technical Library	1
Annapolis, MD 21402	
Commanding Officer	
Naval Ordnance Station	
Attn: Technical Library	1
Indian Head, MD 20640	
Commanding General	
Ballistic Research Laboratory	
Attn: Dr. C. H. Murphy	1
Technical Library	1
Aberdeen Proving Grounds, MD 21005	

DISTRIBUTION (Cont.)

	Copies
Commanding General U.S. Army Missile R&D Command DROMI-TDK Redstone Arsenal	
Attn: Mr. R. Deep	1
Dr. D. J. Spring	1
Technical Library	1
Huntsville, AL 35809	
Commanding Officer Air Force Armament Laboratory	
Attn: Dr. D. Daniel	1
Mr. C. Butler	1
Eglin Air Force Base, FL 32542	
Commanding Officer Air Force Wright Aeronautical Laboratories (AFSC)	
Attn: Dr. G. Kurylowich	1
Mr. D. Shereda	1
Mr. J. Jenskins	1
Wright-Patterson Air Force Base, OH 45433	
NASA Ames Research Center	
Attn: Technical Library	1
Moffett Field, CA 94035	
NASA Langley Research Center	
Attn: Mr. J. South	1
Mr. W. Sawyer	1
Mr C. M. Jackson	1
Technical Library	1
Langley Station Hampton, VA 23365	
Applied Physics Laboratory The Johns Hopkins University	
Attn: Dr. L. L. Cronvich	1
Mr. E. T. Marley	1
Mr. T. Hoye	1
Technical Library	1
Johns Hopkins Road Laurel, MD 20707	

	Copies
General Dynamics Corporation Pomona Division	
Attn: C. Wilcoxson	1
R. Thompson	1
Technical Library	1
P.O. Box 2507 Pomona, CA 91769	
Raytheon Company Missile Systems Division	
Attn: Technical Library	1
Hartwell Road Bedford, MS 01730	
McDonnell-Douglas Astronautics Company (West)	
Attn: Technical Library	1
5301 Bolsa Avenue Huntington Beach, CA 92647	
McDonnell-Douglas Astronautics Company (East)	
Attn: Technical Library	1
Box 516 St. Louis, MO 63166	
Lockheed Missiles and Space Company, Inc.	
Attn: Technical Library	1
P.O. Box 1103 Huntsville, AL 35807	
Lockheed Missiles and Space Company, Inc.	
Attn: Technical Library	1
P.O. Box 504 Sunnyvale, CA 94086	
Nielson Engineering and Research, Inc.	
510 Clyde Avenue Mountain View, CA 95043	1
General Electric Company Armament Systems Department	
Attn: Mr. R. Whyte	1
Burlington, VT 05401	

DISTRIBUTION (Cont.)

	Copies
Hughes Aircraft Corporation Missiles Systems Group Attn: Technical Library Canogo Park, CA 91304	1
Sandia Laboratories Attn: Technical Library Albuquerque, NM 87185	1
Martin Marietta Aerospace Attn: Technical Library P.O. Box 5837 Orlando, FL 32855	1
Honeywell, Inc. Attn: Technical Library 600 Second Street Minneapolis, MN 55343	1
Rockwell International Missile Systems Division Attn: Technical Library 4300 East Fifth Avenue P.O. Box 1259 Columbus, OH 43216	1
Defense Technical Information Center Cameron Station Alexandria, VA 22314	12
Library of Congress Attn: Gift and Exchange Division Washington, DC 20540	2
Internal Distribution:	
K	1
K20	1
K204	10
K21	1
K21 (Mr. T. Pepitone)	1
K21 (Mr. S. Hardy)	1
K22	1
K23	1
K24	1
K24 (Mr. R. Driftmyer)	10
R	1
R40	1
R44	1
G	1
G20	1
G205	1
N20	1
E231	9
E232	3
E06	4

END

2-87

DTIC